SAND78-0962
Unlimited Release

ECONOMIC ANALYSIS OF DARRIEUS VERTICAL AXIS WIND TURBINE SYSTEMS FOR THE GENERATION OF UTILITY GRID ELECTRICAL POWER

VOLUME III - POINT DESIGNS

R. D. Grover, E. G. Kadlec

Prepared by Sandia Laboratories, Albuquerque, New Mexico 87185 and Livermore, California 94550 for the United States Department of Energy under Contract AT(29-1)-789

Printed August 1979

Sandia Laboratories
energy report

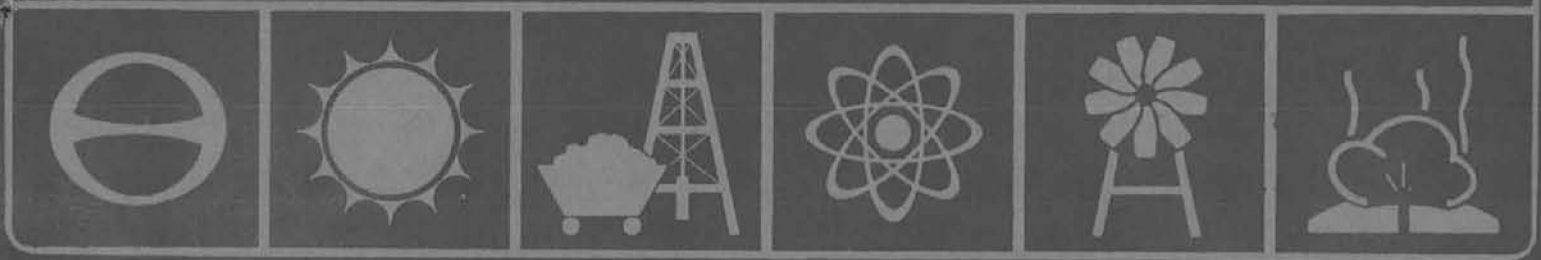

SF 2900-DDB(3-74)

Issued by Sandia Laboratories, operated for the United States Department of Energy by Sandia Corporation.

SAND78-0962

ECONOMIC ANALYSIS OF DARRIEUS VERTICAL-AXIS WIND TURBINE SYSTEMS FOR THE GENERATION OF UTILITY GRID ELECTRICAL POWER

VOLUME III: POINT DESIGNS

Robert D. Grover
Emil G. Kadlec
Advanced Energy Projects Division 4715
Sandia Laboratories
Albuquerque, NM 87185

ABSTRACT

Volume III of this study discusses major features of the Darrieus vertical-axis wind turbine design including the blades, the speed increaser, guy cables and cable anchors, transmission, clutch, brakes, and the electrical system. System weight characteristics are tabulated. The report discusses operation and maintenance costs and requirements and concludes with detailed descriptions of point designs for 120, 200, 500, and 1600-kW Darrieus vertical-axis wind-energy systems. These same point designs are used for the detailed economic analyses discussed in Volume IV.

ACKNOWLEDGMENTS

Special recognition is due J. H. Lackey of Division 2458 for his design efforts and W. N. Sullivan of Division 4715 for his overall direction of this study.

CONTENTS

ILLUSTRATIONS

TABLES

Preface - Objective and Organization of the Vertical Axis Wind Turbine (VAWT) Economic Study

The ultimate objective of the VAWT economic study is to determine as accurately as possible the profitable selling price of Darrieus vertical axis wind energy systems produced by a typical manufacturing and marketing firm. This price may then be compared to the electrical utility energy saved by the system to allow potential users to assess the usefulness of the VAWT concept. The basic approach for assessing the selling price is through a detailed economic analysis of six actual system designs. These designs cover a wide range of system size points, with rotor diameters from 18 to 150 ft, corresponding to approximate peak output ratings from 10 to 1600 kW. All these systems produce 60-Hz utility-line power by means of induction or synchronous generators coupled mechanically to the rotor and electrically to the utility line.

Two independent consultants in parallel conducted the economic analyses of these point designs. A. T. Kearney, Inc., a management consulting firm, provided analyses for the four largest point designs; Alcoa Laboratories considered all six design points. Both studies attempt to determine a reasonable selling price for the various systems at several production rates ranging from 10 to 100 MW of peak power capacity installed annually. In addition, the consultants also estimated the costs of constructing one or four preproduction prototypes of each point design. Toward this objective, the consultants considered a hypothetical company to procure components; perform necessary manufacturing; and manage the sales, marketing, delivery, and field assembly of the units. Profits, overhead, and administrative costs for this hypothetical company are included in estimating the appropriate selling price for each point design.

Sandia Laboratories selected the basic configurations of the point designs (i.e., the number of blades, blade chord, rotor speed, etc) and developed specifications for the configurations using an economic optimization model that reflects the state-of-the-art in Darrieus system design. The computer-adapted optimization model uses mathematical approximations for the costs of major system elements and the energy collection performance of the system. The model effects cost vs performance tradeoffs to identify combinations of system parameters that are both technically feasible and economically optimal.

System configurations identified by the optimization model served as a starting point for all the point designs. Sandia Laboratories completed the designs for the four largest systems (120, 200, 500, and 1600 kW) and Alcoa Laboratories prepared the two smallest systems (10 and 30 kW). The level of detail associated with each design

is commensurate with an adequate determination of component costs and not necessarily with what is required for actual construction of the systems.

This final report is divided into four separate volumes, corresponding to overall organization of the study:

Volume I	The Executive Summary - presents overall conclusions and summarizes key results.
Volume II	Describes the economic optimization model including details of system performance calculations and cost formulas used in the optimization process. The model-estimated costs per kilowatt hour of the optimized systems are presented as a function of the rotor diameter, and the dominant cost and performance factors influencing the results are discussed. The volume concludes with a tabulation of optimized performance and physical characteristics of the point designs.
Volume III	Presents the actual point designs and discusses major design features. Tabular data on energy production, component weights, and component specifications are included.
Volume IV	Summarizes results provided by the cost consultants' analyses, interprets observed trends, and compares results with those from the economic optimization model.

ECONOMIC ANALYSIS OF DARRIEUS VERTICAL-AXIS
WIND TURBINE SYSTEMS FOR THE GENERATION
OF UTILITY GRID ELECTRICAL POWER

VOLUME III: POINT DESIGNS

Introduction

To yield credible results, any study or investigation must be based on reliable information. Certainly the economic feasibility assessment of the Wind Energy Conversion System (WECS) is an endeavor of this type. The concept of pricing actual point designs is used to develop realistic cost data for this assessment. This portion of the final report (Volume III) presents the approach used for these designs, the designs themselves, and some general design analyses.

Six point designs* were generated from the system characteristics established using the economic optimization model described in Volume II. These designs cover a spectrum of sizes (18- to 150-ft diameters) and outputs (10 to 1600 kW). All the designs are for synchronous (constant rpm) rotor control using an induction or synchronous generator connected to an existing utility grid. The ratings used are nominal. A design rationale was established that defined these designs in sufficient detail to allow accurate cost estimates. In turn, this design rationale led to the identification of certain general features shared by this family of turbines. Some of these features were dictated by the original ground rules, others by the economic optimization model, and the rest by the design process itself. The most notable common feature of these point designs is conservative fabrication methods.

Design Rationale

Since VAWT cost estimates are based on point designs, it is imperative that they possess the following qualities:

- Cost/efficiency balance in energy collection and conversion
- Structural soundness
- Longevity
- Reliability of cost estimates
- Low cost

A brief discussion of the design rationale used for each of these categories follows.

*A point design of a VAWT is a design at a specific power point such as 120, 200, 500, or 1600 kW. These points were selected and designs made for a wide range of VAWT sizes to form a basis for cost studies.

Cost/Efficiency Balance

To determine the output of a wind turbine, the characteristic efficiency of the various components must be taken into account. More importantly, costs of efficiency must be assessed and accounted for. This was done for the point designs using the performance/cost relationship embodied in the economic optimization model. In addition, geometry changes imposed by manufacturing/assembling processes can affect the cost/efficiency balance of the design in the actual design process. Attention was given to this aspect throughout the point design process to maintain a reasonable cost/efficiency balance.

Structural Soundness

The Economic Optimization Model processed only those basic configurations and geometries that met or exceeded minimum structural requirements. These structural requirements and the analyses used to determine conformance to these requirements are discussed in length in Volume II and are also included in this volume as Appendix C. The types of analyses used in the model are summarized as follows:

Blades	- Nonlinear finite element static analysis used in dimensional analysis form to determine blade operational stresses and stresses in parked survival wind case.
Tower	- Conventional buckling, load analysis, torsional and bending natural frequency analysis, and analysis of axial stresses.
Tiedowns	- Analysis of cable sag for blade strike and resonant frequency/operating frequency analysis.

The basic structural integrity of the point designs was then maintained or improved during the design process. Conformance to general structural requirements was spot-checked. After completion of the design, the designs were analyzed statically and to some degree dynamically. Hence the designs are judged to be structurally sound for the purposes of this study and only minor changes should be necessary to make a production set of drawings.

Longevity

The point designs incorporate features that either ensure long life (~ 30 yr) or cost-effective replacement. Placing most of the running gear at ground level enhances the ability to "design in" cost-effective replacement.

Reliability of Cost Estimates

Because the success of this overall study largely depends on generating reliable information, the point designs were done to assure easy, reliable cost estimates.

Using catalog items wherever possible instead of specially designed items and simple established fabrication techniques eases the cost-estimating process. As a result, cost estimators were able to apply quotations from fabricators and suppliers to form a reliable basis for component costs and, subsequently, total system costs.

Low Cost

When a choice of approaches was possible, the lowest-cost method of fabrication was chosen. As an example, aluminum extruded blades were chosen for use throughout the point designs because that fabrication method produced blades that were structurally sound, long-lived, reliably cost-estimated, and relatively low-cost. Thus while extruded blades may not be the lowest cost per se, they represent the lowest cost that currently satisfies the other requirements as well. The point designs therefore represent current state-of-the-art turbine design.

General Features

Because of the original guidelines established and the elements of the design rationale used, the point designs share some general features. This section discusses those general features and some of their exceptions.

Blades

All point designs have two extruded aluminum blades with a NACA 0015 cross section and uniform wall thickness. Blades for the largest turbines were designed with multiple longitudinal sections for ease of shipping and assembly. Because of extruding limitations, any blade cross section with a chord greater than 29 in. is made up of two or more extrusions having a longitudinal weld.

The blade shape is a straight-circular arc-straight approximation of a troposkien,[1,2] a configuration that minimizes the amount of blade bending required during fabrication. This shape retains most structural advantages of the troposkien and at the same time substantially reduces fabrication costs.

All the point designs have a height-to-diameter (H/D) ratio of 1.5. The economic optimization model actually indicated a very modest cost-of-energy dependence for H/D ratios between 1.0 and 1.5. The target H/D ratio was selected for the point design to minimize the curved section curvature that eases fabrication and shipping of the blade.

The blades are rigidly attached to the central tower using steel clamps that envelop the blade section. The blade material is 6063 at a T5 temper. Temper is

assumed to be achievable in the as-extruded condition, without any additional heat treatment.

Rotor Central Tower

The central tower transmits torque from the blades and reacts the axial load from the tiedown cables.

A large diameter, thin-wall tower is characteristic in each point design. This is a low weight design and amenable to mass production using spiral welding automatic machinery.

Speed Increaser

The speed increaser used for all point designs consists of an enclosed gear box with controlled lubrication. For overall economy and longevity, an earlier study[3] concluded that an enclosed gear-speed increaser offered the required longevity with minimum maintenance.

These increasers, which have a vertical low-speed shaft and a horizontal high-speed shaft, are catalog items except that the capacity of the thrust bearing in the low-speed shaft must be increased. Increasing this thrust capacity allows the speed increaser to be used as a turbine base and eliminates the need for a separate base and thrust bearing.

Universal Joint

Each point design incorporated a universal joint in the drive train just above the low-speed shaft of the speed increaser. This joint allows for misalignment of the rotor tower with respect to the speed increaser. The joint also allows erection of the turbine after complete assembly without the use of a crane by acting as a hinge.

Guy Cables and Anchors

A three-cable guy configuration is used on all point designs for economic reasons. Since soil conditions were not known, a conservative dead weight/friction approach was used to design the guy-cable anchors. Cost estimates based on this design yield an upper bound. A recently completed foundation and anchor study[4] has identified anchor designs of significantly lower cost than those used on the point designs.

Brakes

Each system has a brake designed to stop the wind turbine for a design condition of 20% overspeed from the rotor synchronous rpm with maximum torque wind loading. A disk brake using standard heavy equipment calipers was chosen.

Electrical Systems

Electrical systems are grid-connected, 3-phase, 480-V or 4160-V outputs.

The 10-, 30-, and 120-kW systems have a 480-V, 3-phase output with 480-V controls, whereas the 200- and 500-kW systems achieve a 4160-V output by using 480-V machinery and controls and a step-up transformer. The 1600-kW system uses 4160-V controls and machinery.

The 10-, 30-, and 120-kW systems use induction machinery. The 200-, 500-, and 1600-kW systems have two options; option 1 is a synchronous machinery system, while option 2 is an induction machinery system.

The 10- and 30-kW systems use the induction machine for starting with full voltage. The 120-kW system options include the induction machine with full voltage start and the use of a clutch. The 200- and 500-kW systems with option 2 use the induction machine with reduced voltage during startup. The 1600-kW option 2 induction system is brought up to speed under no-load with subsequent mechanical clutching to start the rotor; the 200-, 500-, and 1600-kW option 1 synchronous systems operate the same way.

System Weight Characteristics

Point design weights listed in Table I are the calculated weights of the actual point designs as opposed to the weight estimates generated by the Economic Optimization Model discussed in Volume II. Table I lists weights by components such as blades, tower, tiedowns, transmission, and generator. The weight of mounting hardware, clamps, bearings, etc., is included in the total component weight as appropriate.

In addition, weight estimates of the four machines optimized to operate in 12- and 18-mph average windspeed sites are listed at the bottom of Table I. These estimates were made by changing point design weights to account for the appropriate transmission, generator, and structural requirements. The nominal rating of these machines is changed when optimized for these windspeeds.

System output vs weight is presented in Table II. Expected annual output for each system is calculated for various windspeeds. The turbine as optimized for 15-mph average windspeed is operated at 12-, 15-, and 18-mph average conditions. These outputs are compared to the outputs of turbines optimized for 12- and 18-mph average conditions.

Note that the energy per unit weight is very sensitive to site wind conditions but ostensibly not sensitive to turbine optimization for the range presented.

TABLE I

Point Design Weights by Component Optimized for 15-mph Average Windspeed

Nominal Rating (kW)	10	30	120	200	500	1600
	Weight (lb) (Followed by Percentage of Total Weight)					
Blades	310(21)	1120(23)	5040(28)	9190(23)	20,000(21)	69,710(25)
Tower	260(18)	1600(32)	5200(29)	13,720(34)	29,330(31)	102,390(36)
Tiedowns	270(19)	751(15)	3850(21)	8335(20)	15,960(17)	48,360(17)
Transmission	200(14)	600(12)	2000(11)	5250(13)	21,800(23)	46,000(16)
Generator	160(11)	400(8)	1260(7)	2370(6)	3830(4)	10,600(4)
Other	250(17)	500(10)	710(4)	1960(5)	4300(5)	6850(2)
Total	1450	4971	18,070	40,825	95,220	283,910
Total 12-mph Optimum Estimate			17,037	37,224	83,100	265,000
Rating Optimized for Windspeed (kW)			83	140	270	860
Total 18-mph Optimum Estimate			20,862	48,255	112,800	352,000
Rating Optimized for Windspeed (kW)			180	390	870	2500

The range of 10- to 13-kWh/lb compares favorably with the range of current and near-term large horizontal-axis machines, particularly in light of the fact that (as discussed in the design rationale section) these designs represent state-of-the-art capability and simple fabrication methods. The application of value engineering, other fabrication techniques, and advanced development will enhance the energy-to-weight ratio.

Operation and Maintenance

An obvious item in the overall cost structure of a wind turbine is the cost of operation and maintenance (O&M). This section deals with such costs in the context of a mature machine beyond prototype stage.

Maintenance and Inspection Requirements

The bearing at the top of the tower where the guy cables are attached to the turbine should be lubricated at 6-month intervals.

Transmission oil should be changed yearly.

Motor bearings should be lubricated every 6 months.

TABLE II

System Output vs Weight

Nominal Size (Dia x Ht)	Opt. Design Windspeed (mph avg)	Sited Windspeed (mph avg)	Total System Wt(lb)	Nominal Rating (kW)	Output kWh (lb/yr)	Annual Output (kWh)
55 x 83	18	18	20,862	180	20.7	432,000
55 x 83	15	18	18,060	120	20.4	368,000
55 x 83	15	15	18,060	120	13.5	246,000
55 x 83	15	12	18,060	120	7.3	132,000
55 x 83	12	12	17,037	83	7.2	123,000
75 x 113	18	18	48,300	390	18.1	875,000
75 x 113	15	18	40,825	200	17.9	731,000
75 x 113	15	15	40,825	200	11.9	490,000
75 x 113	15	12	40,825	200	6.4	263,000
75 x 113	12	12	37,200	140	7.0	259,000
100 x 150	18	18	112,800	870	16.8	1,890,000
100 x 150	15	18	95,220	500	17.1	1,630,000
100 x 150	15	15	95,220	500	11.2	1,070,000
100 x 150	15	12	95,220	500	5.8	553,000
100 x 150	12	12	83,100	270	6.6	549,000
150 x 225	18	18	352,000	2500	15.1	5,330,000
150 x 225	15	18	283,910	1600	15.4	4,370,000
150 x 225	15	15	283,910	1600	10.4	2,950,000
150 x 225	15	12	283,910	1600	5.6	1,590,000
150 x 225	12	12	265,000	860	6.0	1,580,000

The guy-cable tension should be checked semiannually in June and December and adjusted if necessary. This permits proper cable tension at times other than those of extreme temperature and will give better cable tension for a longer time. Turbine perpendicularity can be checked and corrected if necessary by proper selection of the cables to be tensioned and the amount of cable tensioning performed on each cable.

Although the turbine is designed to operate for a long time with only the above maintenance, it should be visually inspected at the 6-month cable tensioning and lubrication intervals for lubrication leaks; for cracked, broken, and loose parts; and for unusual noises.

The required manpower expenditure ranges from 0.5 man-day per year for the 10-kW system to 10 man-days for the 1.6-MW system. This ranges from

$$\frac{0.5 \times 200}{9000} = 1\% \text{ of } \frac{\text{Initial Cost}}{\text{Year}}$$

$$\text{to } \frac{10 \times 200}{650{,}000} = 0.3\% \text{ of } \frac{\text{Initial Cost}}{\text{Year}}$$

where labor costs are $200 per man-day and consumables are included in labor cost.

Replacement

Although the bearings, generator, and speed increaser are designed for the machine lifetime of 30 years, it is prudent to assume that some fraction of these components will require replacement. For estimating purposes, it is assumed that the wind turbine system will require major servicing that is the equivalent of

- 10% of the turbines requiring bearing replacement
- 10% of the turbines requiring generator/electrical system replacement
- 10% of the turbines requiring speed-increaser replacement

For cost-estimating purposes, a bearing replacement is assumed to cost 50% of the initial erection cost; a generator/electrical system twice the original generator/electrical cost; and a speed increaser replacement 1.5 times the original speed increaser costs.

For a design life of 30 years, and using the system costs in Volume IV, each turbine is assessed annual replacement costs as follows:

$$\frac{\text{Percent Replaced} \times \text{Assessment} \times \text{Fraction of Total IC}}{\text{Turbine Lifetime}}$$

In terms of percent of initial cost (IC) $\frac{\text{IC}}{\%\ \text{year}}$:

Bearings

$$\frac{10 \times 0.50 \times 0.11}{30} = 0.02$$

Generator/Electrical

$$\frac{10 \times 2 \times 0.12}{30} = 0.08$$

Speed Increaser

$$\frac{10 \times 1.5 \times 0.19}{30} = 0.10$$

Total Replacement Assessment 0.20

Operation

The amount of manpower expended for operation is strongly influenced by the application to which the wind turbine is applied and by the type of control system used. For a utility application using an automatic control system, the amount of time charged per turbine is constant with respect to size. Dispatching manpower might be on the order of 15-20 minutes per week. Expressed as an annual cost, this is

$$\frac{20 \times 52 \times 200}{60 \times 8} = \$433$$

Expressed as percent of initial cost,

% IC		
10 kW	200 kW	1600 kW
$\frac{433}{9000} = 4.8$	$\frac{433}{125,000} = 0.35$	$\frac{433}{650,000} = 0.07$

Total O&M Costs

Total O&M cost estimates for three turbine sizes are as follows in terms of percent of initial cost per year:

	% IC per Year		
	10 kW	200 kW	1600 kW
Maintenance and Inspection	1	0.3	0.3
Replacement	0.2	0.2	0.2
Operation	4.8	0.35	0.07
Total O&M	6.0	0.85	0.57

The methodology previously developed can be expanded to produce the following estimates of O&M cases for the point designs.

Annual Maintenance and Operation Costs
(Estimated)

	10 kW	30 kW	120 kW	200 kW	500 kW	1600 kW
Maintenance and Inspection	$100	$150	$200	$ 400	$1000	$2000
Replacement	18	30	140	250	580	1300
Operation	433	433	433	433	433	433
Total	$551	$613	$733	$1083	$2013	$3733
Installed Costs	$9000	$15,000	$70,000	$125,000	$290,000	$650,000

Point Design Descriptions

As previously discussed, the Economic Optimization Model was used to identify potential point designs. These potential designs were then worked into actual designs in sufficient detail to permit both analysis and cost estimation.

One of these designs (120 kW) is presented in detail in the following section. The remaining designs are briefly discussed, along with erection schemes for the 500 kW design. Detailed drawings and specifications of the point designs are cataloged in Appendix A.

Mechanical Design - 120-kW VAWT (Drawing No. S26580)

The characteristics calculated using the Economic Optimization Model are presented in Table III.

Blades -- The blades are 82.5 ft high and 55 ft in diameter at the blade centerline, for a height-to-diameter (H/D) ratio of 1.5 to 1. Figure 1 shows a troposkien blade shape for a VAWT with this H/D ratio. Since such a shape is difficult to manufacture, an approximation of the troposkien with a circular-arc/straight-line shape is used for the blade design shown in Fig. 2 (Ref. 1). Figure 3 shows the geometry of the VAWT in the two-bladed configuration.

The airfoil shape of the blade is a NACA 0015 with a chord length of 24.24 in. and a blade length of 24 in. Figure 4 shows the blade cross-sectional design. The blade is a 6063-T5 aluminum extrusion. Each blade section is a single extrusion, with the curved section shaped from a straight extrusion using incremental three-point bending.

The blade length is comprised of one curved section and two straight sections joined together before the blade is assembled to the VAWT shaft. Building the blades in three shorter sections makes shipping them easier.

TABLE III

Estimated Design Features - 120-kW System

Actual Rating	Dia. (ft)	H/D Ratio	Steel Tower Dia. (ft)	Steel Tower Wall Thickness (in.)	Tiedowns (3) Length (ft)	Tiedowns (3) Cable Area ($in.^2$)	Tiedowns (3) Pretension (lb)	Blades (2) Chord (in.)	Blades (2) Wall Thickness (in.)
116 kW @ 31 mph, Design rpm: 52	55	1.5	3.7	0.060	175	1.0	20,000	24.0	0.24

Drive-Train Torques (lb-ft)

Condition	High-Speed Shaft (1800 rpm)	Low-Speed Shaft (Rotor rpm)	Duty Cycle
Normal Operating	510	17,600	300 h/yr, continuous
Runaway to 63 rpm and Emergency Braking	880	-30,400	Single use without permanent damage to drive train
Starting	NA	NA	360 starts/yr

System Performance @ 52 rpm ($0.076\ lbm/ft^3$ air density)

Windspeed (mph) At 30 ft. Ht.	Windspeed (mph) At Turbine Centerline	Turbine Output (kW)	Electrical Output (kW)
9	9.9	2.0	-----
10	11.0	4.7	-----
12	13.1	11.7	1.4
14	15.3	20.7	10.5
16	17.5	31.8	21.5
18	19.7	44.5	34.1
20	21.9	57.9	47.3
22	24.1	71.8	60.8
24	26.3	85.8	74.2
26	28.5	99.5	87.2
28	30.7	112.5	99.5
30	32.9	124.5	110.9
31	34.0	130.0	116.0
32	35.0	128.0	114.0
34	37.2	124.2	110.4
36	39.4	120.7	107.2
38	41.6	117.4	104.2
40	43.8	114.5	101.4

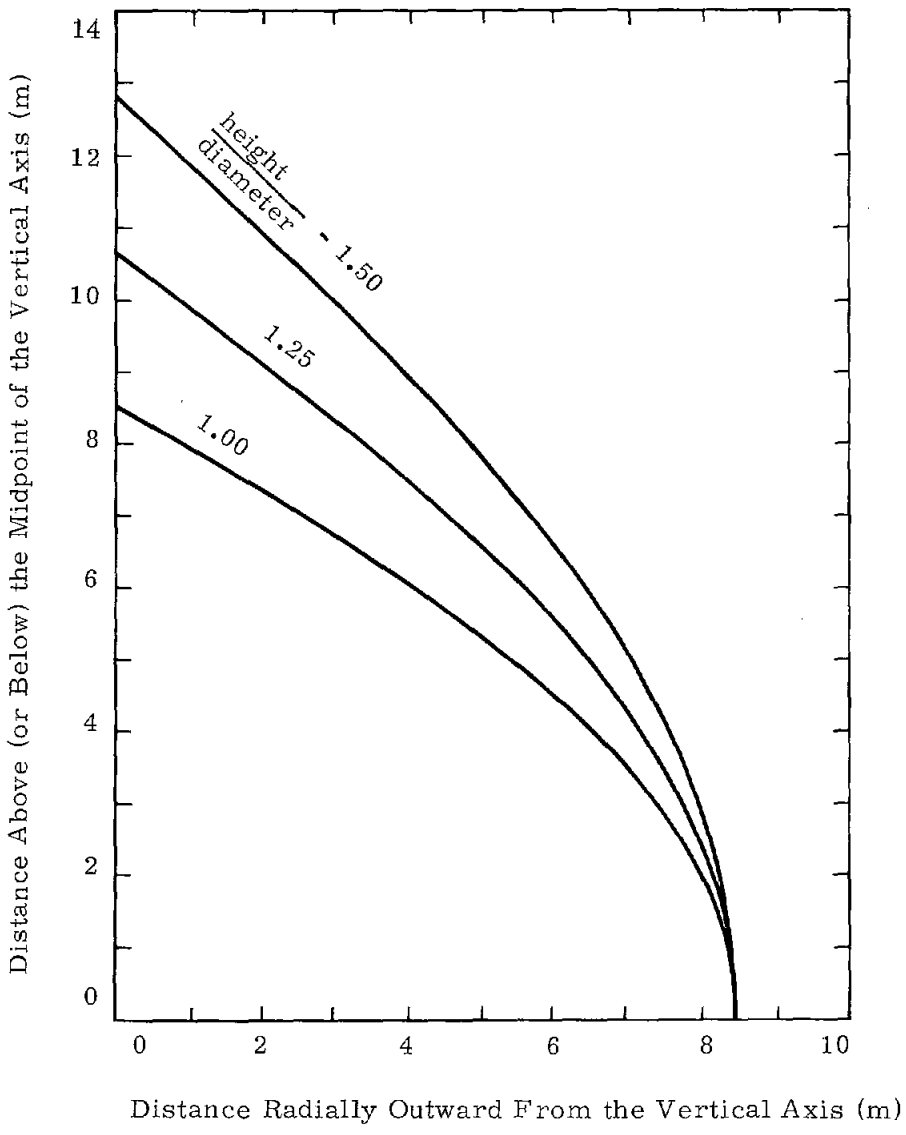

Figure 1. Troposkien Blade Shapes

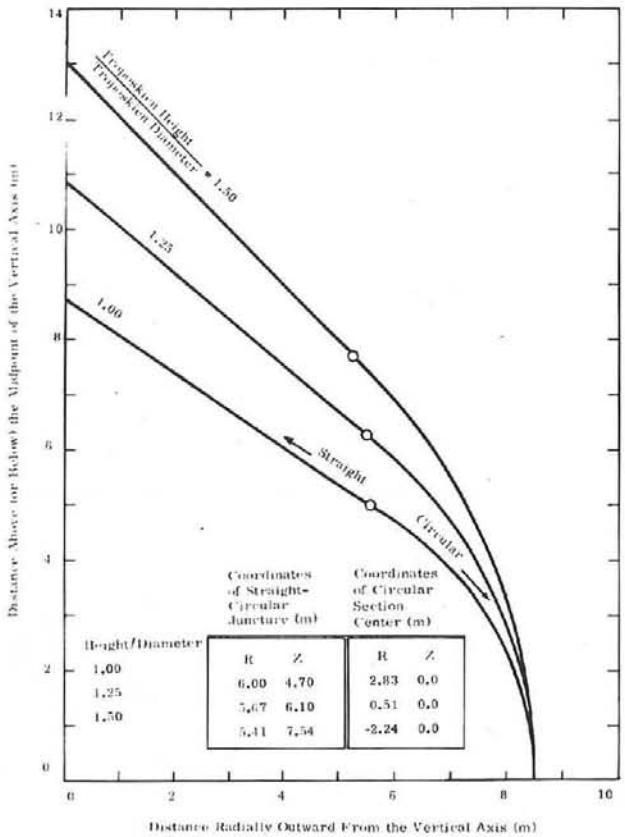

Figure 2. Circular-Arc - Straight-Line Blade Shape Approximation of Troposkiens

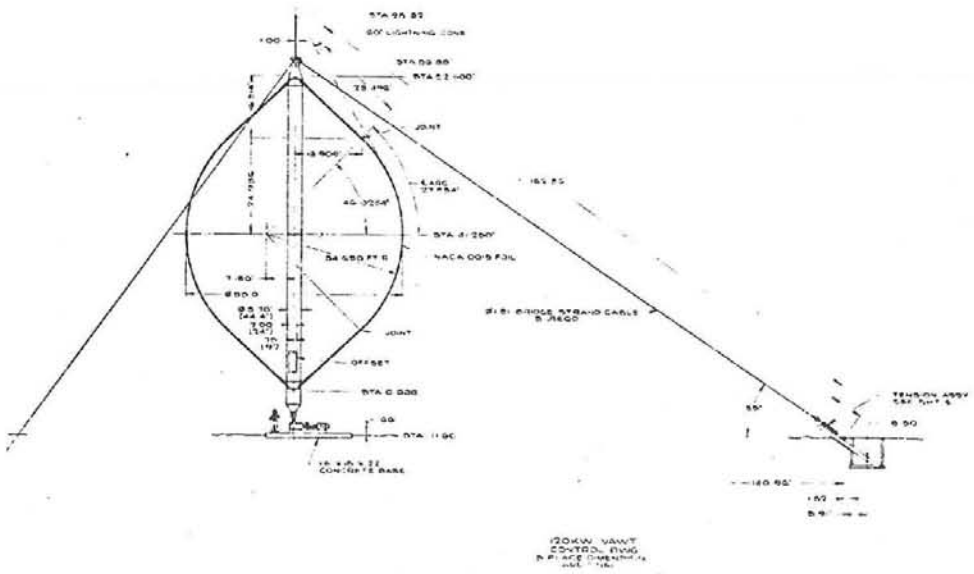

Figure 3. 120-kW VAWT Shape

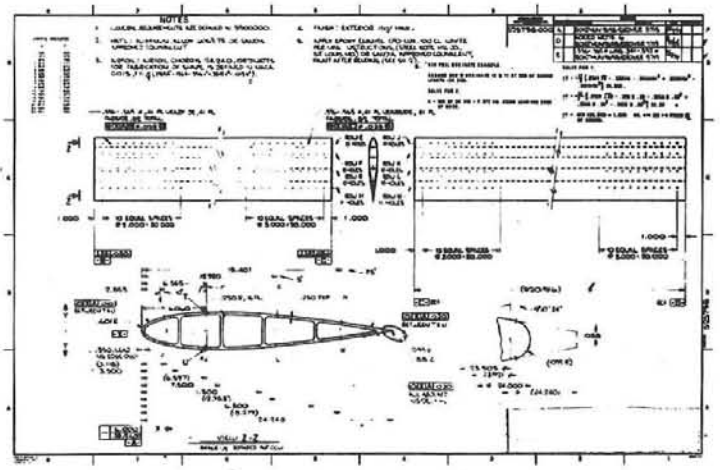

Figure 4. 120-kW VAWT Blade Design

The blade sections are joined together with aluminum extrusions placed into the blade cavities and riveted to achieve a smooth aerodynamic surface on the blade exterior in the joint area (Fig. 5). The blade is attached to the VAWT shaft by bolting

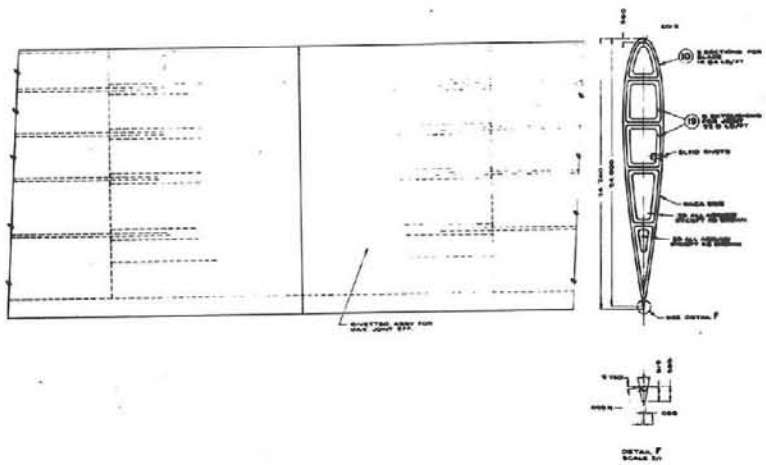

Figure 5. 120-kW VAWT Blade Joint Design

cheek plates on both sides of the blade and then to the shaft (Fig. 6). Disruption

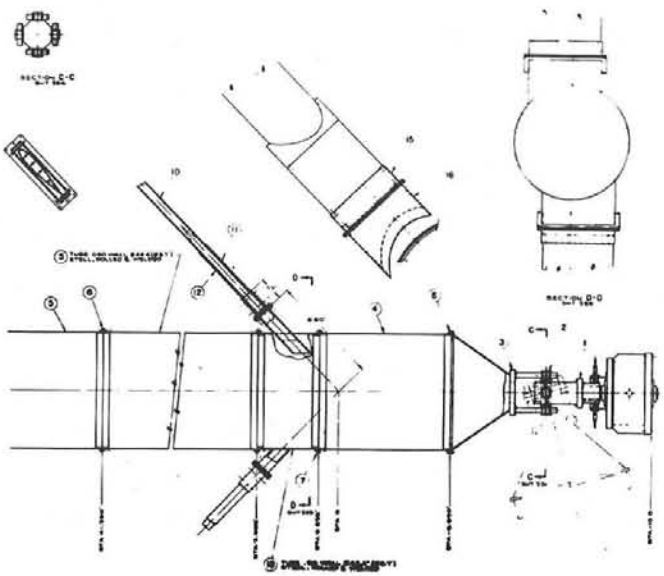

Figure 6. 120-kW Blade Attachment Design

of the blade aerodynamic surface near the shaft by the cheek plates is of little consequence because of the low blade velocity in this area. This arrangement more easily supports the blade root loads.

Guy Cables -- The VAWT is supported by three guy cables attached to the top of the VAWT (Fig. 7) and anchored at ground level (Fig. 8). Bridge strand with an effec-

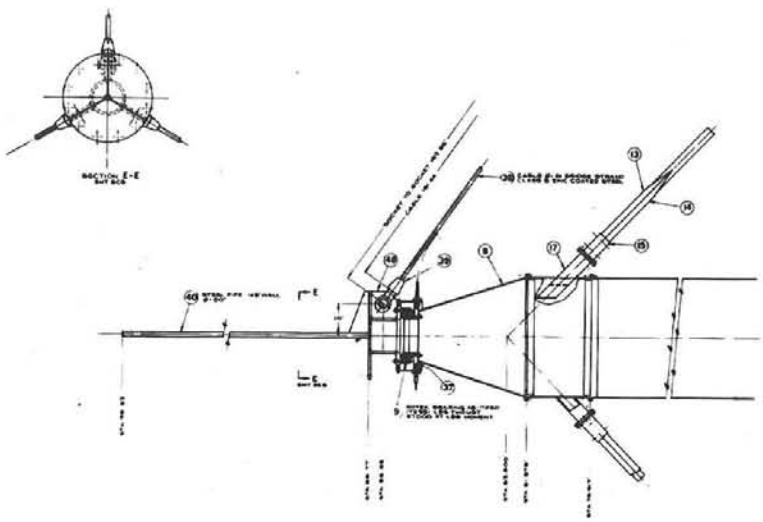

Figure 7. 120-kW VAWT Guy-Cable Attachment Design

tive modulus of elasticity of 23,000,000 psi was selected for the guy cables to achieve cable rigidity for resonant frequency control. The pretension load in the guy cables is 20,000 lb. The 1.3-in.-diameter cable, selected on the criterion of rigidity, has a strength of 208,000 lb. A Class B zinc-cable coating was thought to be generally sufficient protection, although a Class C zinc coating could be used in extreme environments such as areas near the ocean.

The bearing at the top of the VAWT must support the guy-cable forces as well as the nonrotating material above the bearing. A Rotek bearing was selected for this position because of its capability to react to thrust, radial, and moment loads simultaneously with a single bearing.

Transmission -- Building the VAWT directly upon the transmission is the most economical mounting method because it uses an existing transmission bearing (Fig. 9). Load at the transmission can be determined when the VAWT blade and tower weights and

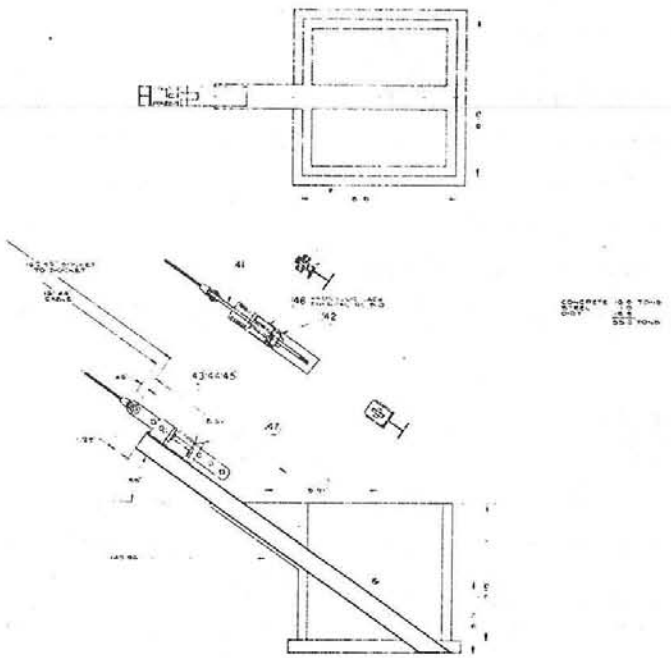

Figure 8. 120-kW VAWT Guy-Cable Tiedown Design

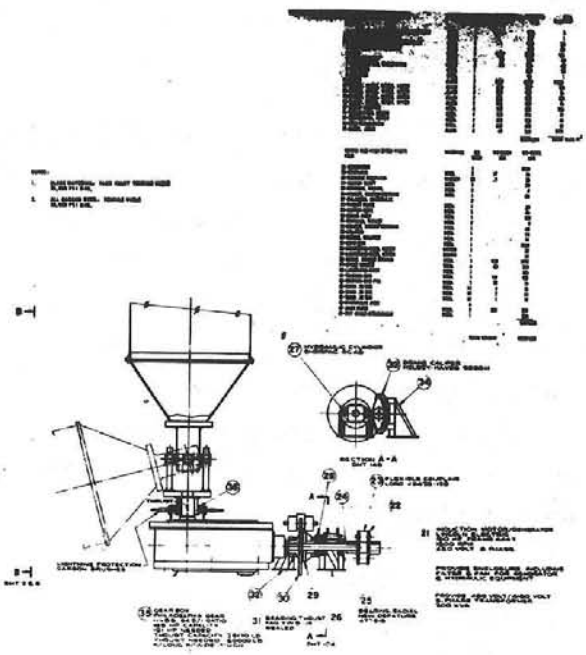

Figure 9. 120-kW Transmission Brake and Clutch Design

guy-cable tension are known. A transmission can then be selected to carry this load and transmit power to the generator.

A Philadelphia Gear transmission with a gear ratio of 34.5 to 1 was selected for proper power-transmission capability, for adapting to an 1800-rpm electric generator. The thrust load capability, however, is only about one-half the capability needed. It is assumed that a bearing of the proper size can be incorporated in the transmission; otherwise a lower support tower is necessary to carry the VAWT. The gear ratio is not exactly correct, but slight changes can be made when ordering the transmission.

Clutch -- A VAWT cannot be reliably started by the wind; it must be started by an outside source such as a motor. The generator can be used as a starting motor if the motor is allowed to operate at full speed during startup. This is done by running the motor at full speed and using a clutch to engage and start the VAWT. While producing the rated torque, the clutch is allowed to slip until the VAWT is up to rated speed. This prevents motor and drive-train overload as might be experienced if the VAWT were connected directly to the motor during motor start.

The electric motor is started, brought up to full speed, and synchronized with the grid in the case of a synchronous motor. The clutch, which is engaged by a hydraulic cylinder, slips until the VAWT is brought up to rated speed with the clutch providing rated torque.

See Appendix B for clutch design calculations.

Brake -- The brake disk is designed by the same method as the clutch. The amount of energy that must be absorbed to stop the turbine is determined and the brake area can be calculated. Table III shows that runaway torque due to wind is 30,400 lb-ft at a turbine speed of 63 rpm. Inertial energy of the turbine at 63 rpm is 832,000 ft-lb; the energy due to the wind during stopping is determined by the selected stopping torque of the brake upon the turbine. Brake torque must exceed 30,400 lb-ft of wind torque to slow the turbine. A brake torque of 45,000 lb-ft is selected as reasonable because the turbine and transmission must be designed to stop the turbine one time without damage in an engineered stop. To determine stop time at a brake torque of 45,000 lb-ft, the inertial energy must be absorbed at the same time as the wind energy.

See Appendix B for brake design calculations.

Cable Anchors -- The tiedown cable anchors were designed for a worst case in which the anchors are built on top of the ground. A coefficient of friction of 0.3 was used for the anchor on the ground and no allowance was used for ground shear for a buried

anchor. The anchor, formed with two internal cavities for ballast space, was sized as though the cavities were filled with dirt.

Other cable-anchoring systems should be considered for specific sites during the site study before building a VAWT.

Cable tension is achieved with hydraulic cylinders. After the desired tension is achieved, an electric motor screws a nut into position to maintain the tension. With proper sensing and control of the hydraulic system and the electric motor, this system could be used for an automatic cable tensioning system.

Mechanical Design - 200-kW VAWT

Drawing S25325 in Appendix A shows the mechanical design of the 200-kW VAWT. The rating of this VAWT is 220 kW at a speed of 41 rpm in a 31-mph wind.

Blades, Guy Cables, Transmission, Clutch, and Brake -- The blades are 112.5 ft high and 75 ft in diameter, for an H/D ratio of 1.5. The blades are divided into four sections -- two straight and two curved. The curved portion of the blade is divided into two sections to achieve a reasonable shipping length.

The airfoil shape of the blade is a NACA 0015 with a chord length of 29 in. The blade is a 6063-T5 aluminum extrusion. Each blade section is a single extrusion, with the curved section formed from a straight extrusion into the curved shape.

Aluminum extrusions placed into the blade cavities and riveted to the blade join the sections together. The blade is attached to the VAWT shaft by bolting cheek plates onto both sides of the blade and then to the shaft.

The VAWT is supported by three guy cables attached to the top and to anchors at ground level. Guy-cable pretension for this VAWT is 46,000 lb. The cable selected is a 1.8-in.-diameter Class B zinc-coated bridge strand with a breaking strength of 396,000 lb.

A Rotek bearing was selected for the top of the VAWT because of its capability to react thrust, radial, and moment loads simultaneously with a single bearing.

The VAWT is built directly upon the transmission shaft. A Philadelphia Gear transmission was selected for proper power-transmission capability and nearly proper gear ratio, but the thrust-bearing capability is only about one-half that required.

The clutch for starting the VAWT is mounted on top of a differential. To start the VAWT, the generator is used as a motor and the motor is brought up to full operating speed. At this time the motor turns the differential and the clutch turns freely.

The brake caliper at the clutch plate applies a force to the plate as hydraulic pressure is applied to the caliper, gradually stopping the clutch plate. In turn the VAWT starts to rotate and accelerates to full speed. The clutch plate absorbs the heat of friction caused by the caliper during startup. The VAWT is started at the rated torque of 42,000 lb-ft in 13 seconds; the clutch plate must absorb 1.2×10^6 ft-lb or 1540 Btu of energy.

The brake for stopping the VAWT is located on the differential shaft between the differential and the generator. The runaway torque for the VAWT is 75,000 lb-ft and a brake torque of 110,000 lb-ft was selected to stop the VAWT. This requires a stopping time of 19 seconds and an energy absorption capability in the brake disk of 5.4×10^6 ft-lb, or 6944 Btu.

Cable Anchors -- The tiedown cable anchors were designed for a worst case in which the anchors are built on top of the ground. A coefficient of friction of 0.3 was used for the anchor on the ground and no allowance was used for ground shear for a buried anchor. The anchor, formed with two internal cavities for ballast space, was sized as though the cavities were filled with dirt.

Other cable-anchoring systems should be considered for specific sites during the site study before building a VAWT.

Cable tension is achieved with hydraulic cylinders. After the desired tension is achieved, an electric motor screws a nut into position to maintain the tension. With proper sensing and control of the hydraulic system and the electric motor, this system could be used for an automatic cable tensioning system.

Mechanical Design - 500-kW VAWT

Drawing S24633 in Appendix A shows the mechanical design of the 500-kW VAWT. The rating of this VAWT is 482 kW at a speed of 30.8 rpm in a 31-mph wind.

Blades, Guy Cables, Transmission, Clutch, and Brake -- The blades are 150 ft high and 100 ft in diameter, for an H/D ratio of 1.5. The blades are divided into four sections -- two straight and two curved. The curved portion of the blade is divided into two sections to achieve a reasonable shipping length.

The airfoil shape of the blade is a NACA 0015 with a chord length of 43 in. The blade is extruded with 6063-T5 aluminum. The largest blade chord that can be extruded is 29 in. The 43-in. chord of the blade is extruded in two pieces and put together with a modified tongue-and-groove joint. After the two pieces are put together to form the 43-in. airfoil shape, the curved sections are formed.

Aluminum extrusions placed into the blade cavities and riveted to the blade join the blade sections together. The blade is attached to the VAWT shaft by bolting cheek plates onto both sides of the blade and then to the shaft.

The VAWT is supported by three guy cables attached to the top and to anchors at ground level. Guy-cable pretension for this VAWT is 86,000 lb. The cable selected is a 2.3-in.-diameter Class B zinc-coated bridge strand with a breaking strength of 644,000 lb.

A Rotek bearing was selected for the top of the VAWT because of its capability to react to thrust, radial, and moment loads simultaneously with a single bearing.

The VAWT is built directly upon the transmission shaft. A Philadelphia Gear transmission was selected for proper power-transmission capability and nearly proper gear ratio, but the thrust-bearing capability is only about one-half that required.

The clutch for starting the VAWT is mounted on top of a differential. To start the VAWT, the generator is used as a motor and the motor is brought up to full operating speed. At this time the motor turns the differential and the clutch turns freely. The brake caliper at the clutch plate applies a force to the plate as hydraulic pressure is applied to the caliper, gradually stopping the clutch plate. In turn, the VAWT starts to rotate and accelerates to full speed. The clutch plate absorbs the heat of friction caused by the caliper during startup. The VAWT is started at the rated torque of 121,300 lb-ft in 13 seconds; the clutch plate must absorb 2.44×10^6 ft-lb, or 3100 Btu of energy.

The brake for stopping the VAWT is located on the differential shaft between the differential and the generator. The runaway torque for the VAWT is 210,000 lb-ft, and a brake torque of 300,000 lb-ft was selected to stop the VAWT. This requires a stopping time of 20 seconds and an energy absorption capability in the brake disk of 11.3×10^6 ft-lb or 14,540 Btu.

Cable Anchors -- The tiedown cable anchors were designed for a worst case in which the anchors are built on top of the ground. A coefficient of friction of 0.3 was used for the anchor on the ground and no allowance was used for ground shear for a buried anchor. The anchor, formed with two internal cavities for ballast space, was sized as though the cavities were filled with dirt.

Other cable-anchoring systems should be considered for specific sites during the site study before building a VAWT.

Cable tension is achieved with hydraulic cylinders. After the desired tension is achieved, an electric motor screws a nut into position to maintain the tension. With

proper sensing and control of the hydraulic system and the electric motor, this system could be used for an automatic cable tensioning system.

Mechanical Design - 1600-kW Design

Drawing S25603 in Appendix A shows the mechanical design of the 1600-kW VAWT. The rating of this VAWT is 1650-kW at a speed of 22.1 rpm in a 32-mph wind.

Blades, Guy Cables, Transmission, Clutch, and Brake -- The blades are 225 ft high and 150 ft in diameter for an H/D ratio of 1.5. The blades are divided into five sections -- two straight and three curved. The curved portion of the blade is divided into three sections to achieve a reasonable shipping length and arc height.

The airfoil shape of the blade is a NACA 0015 with a chord length of 64.5 in. The blade is extruded with 6063-T5 aluminum. The 64.5-in. chord of the blade is extruded in three pieces and put together with a modified tongue-and-groove joint. After the three pieces are put together to form the 64.5 in. airfoil shape, the curved sections are formed.

Aluminum extrusions placed into the blade cavities and riveted to the blade join the blade sections together. The blade is attached to the VAWT shaft by bolting cheek plates onto both sides of the blade and then to the shaft.

The VAWT is supported by three guy cables attached to the top and to anchors at ground level. Guy-cable pretension for this VAWT is 231,000 lb. The cable selected is a 3.4-in.-diameter Class B zinc-coated bridge strand with a breaking strength of 1,326,000 lb.

A Rotek bearing was selected for the top of the VAWT because of its capability to react thrust, radial, and moment loads simultaneously with a single bearing.

The VAWT is built directly upon the transmission shaft. A Philadelphia Gear transmission was selected for proper power-transmission capability and nearly proper gear ratio, but the thrust-bearing capability is only about one-half that required.

The clutch for starting the VAWT is mounted between the generator and the transmission. To start the VAWT, the generator is used as a motor and the motor is brought up to full operating speed. The clutch, which slips during startup, is designed to absorb frictional heat. The VAWT is started at the rated torque of 554,000 lb-ft in 18 seconds; the clutch plate must absorb 11.5×10^6 ft-lb, or 14,830 Btu of energy.

The brake for stopping the VAWT is located between the transmission and the generator. The runaway torque for the VAWT is 1×10^6 lb-ft, and a brake torque of 1.5×10^6 lb-ft was selected to stop the VAWT. This requires a stopping time of 27 seconds and an energy absorption capability in the brake disk of 47×10^6 ft-lb, or 60,400 Btu.

Cable Anchors -- The tiedown cable anchors were designed for a worst case in which the anchors are built on top of the ground. A coefficient of friction of .3 was used for the anchor on the ground and no allowance was used for ground shear for a buried anchor. The anchor, formed with two internal cavities for ballast space, was sized as though the cavities were filled with dirt.

Other cable-anchoring systems should be considered for specific sites during the site study before building a VAWT.

Cable tension is achieved with hydraulic cylinders. After the desired tension is achieved, an electric motor screws a nut into position to maintain the tension. With proper sensing and control of the hydraulic system and the electric motor, this system could be used for an automatic cable tensioning system.

Figure 10 (Drawing no. S25070) is the design of a method for lifting the 500-kW

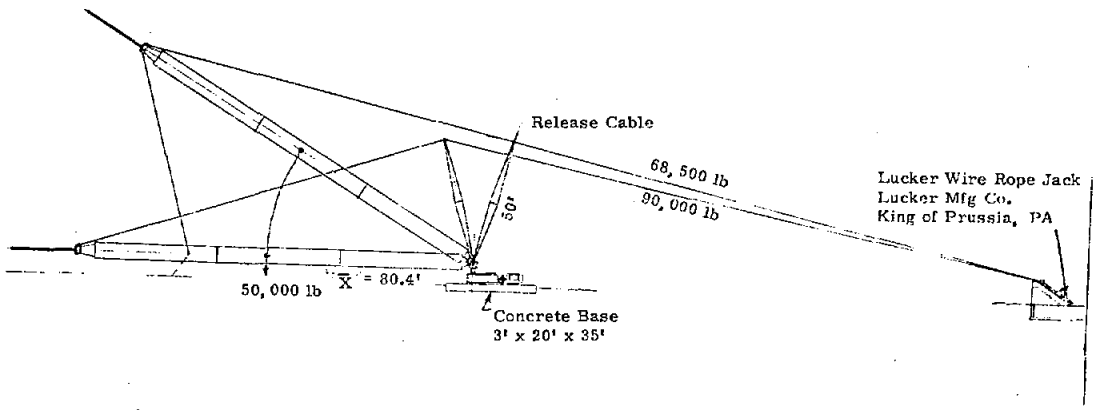

Figure 10. Gin Pole Erection System

VAWT into the vertical position using a gin pole and a power source; Fig. 11 (Drawing no. S25070) is the design for lifting the 500-kW VAWT into the vertical position using a hydraulic cylinder and a power source.

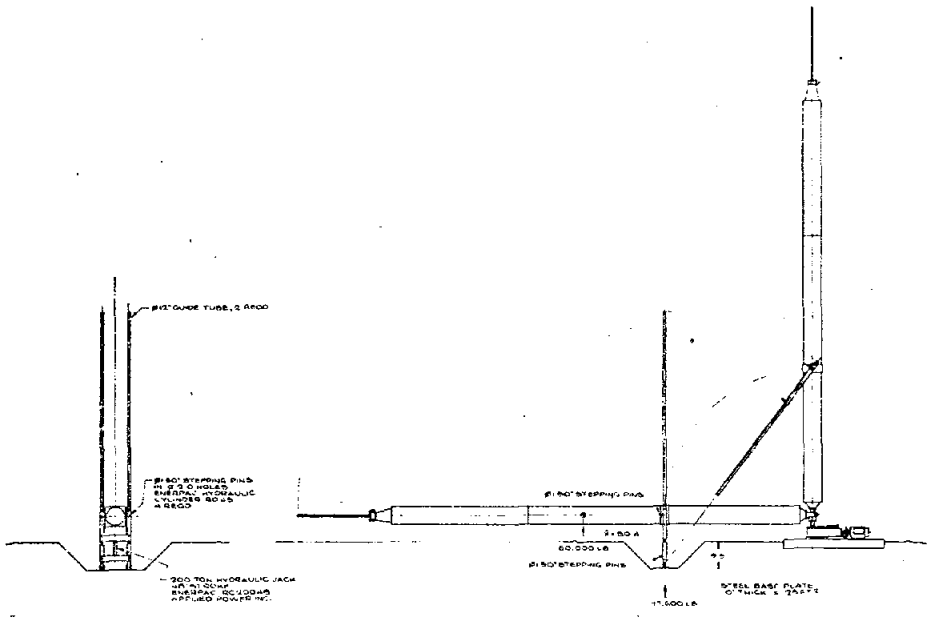

Figure 11. Hydraulic Erection System

APPENDIX A

Point Design Tabulations and Drawings

120-kW Drawing No. S26580
200-kW Drawing No. S25325
500-kW Drawing No. S24633
1600-kW Drawing No. S25603

TABLE A-I

Design Features - 200-kW System
(Single Pass, 29-in. Chord Extrusions)
(Figures A-1 through A-7)

Actual Rating	Dia. (ft)	H/D Ratio	Steel Tower Dia. (ft)	Steel Tower Wall Thickness (in.)	Steel Tower Weight (lb)	Tiedowns (3) Length (ft)	Tiedowns (3) Cable Area ($in.^2$)	Tiedowns (3) Tiedown Weight (lb)	Blades (2) Chord (in.)	Blades (2) Straight Section Length (ft)	Blades (2) Curved Section Length (ft)	Blades (2) Per-Blade Weight (lb) (incl. joints)
226 kW @ 31 mph	75	1.5	4.7	0.090	6000	250	1.9	4982	29	32.2	73.4	31.49

1st Torsion Freq. - 18.3 Hz
1st Bending Freq. - 3.4 Hz

Pretension - 46,000 lb
1st Tiedown Freq. - 0.94 Hz

Blade Wall Thickness - 0.25 in.
Number of Joints - 3
Total Weight of Joints - 705 lb

Drive-Train Torques (lb-ft)

Condition	High-Speed Shaft (1800 rpm)	Rotor Shaft (Rotor rpm)	Service Factor	Duty Cycle
Normal Operating	1000	45,200	1.2	3000 h/yr, continuous
Startup	-1000	-45,200	1.0	360 starts/yr
Runaway to 50 rpm and Emergency Braking	1670	75,000	1.0	Single use without permanent damage to drive train

System Performance @ 31 rpm
(0.076 lbm/ft^3 air density)

Windspeed (mph) At 30 ft Ht	Windspeed (mph) At Turbine Centerline	Turbine Output (kW)	Electrical Output (kW)
8	9.3	1.6	-----
10	11.6	12.3	-----
12	14.0	27.0	3.1
14	16.3	45.5	21.6
16	18.6	67.6	43.5
18	20.9	92.1	67.5
20	23.3	118.2	93.4
22	25.6	145.4	119.9
24	27.9	173.1	146.5
26	30.3	200.7	173.0
28	32.6	227.7	198.5
30	34.9	253.4	222.8
31	36.1	265.8	226.0
32	37.2	252.8	222.3
34	39.6	245.2	215.1
36	41.9	238.3	208.7
38	44.2	232.0	202.7
40	46.6	226.1	197.1

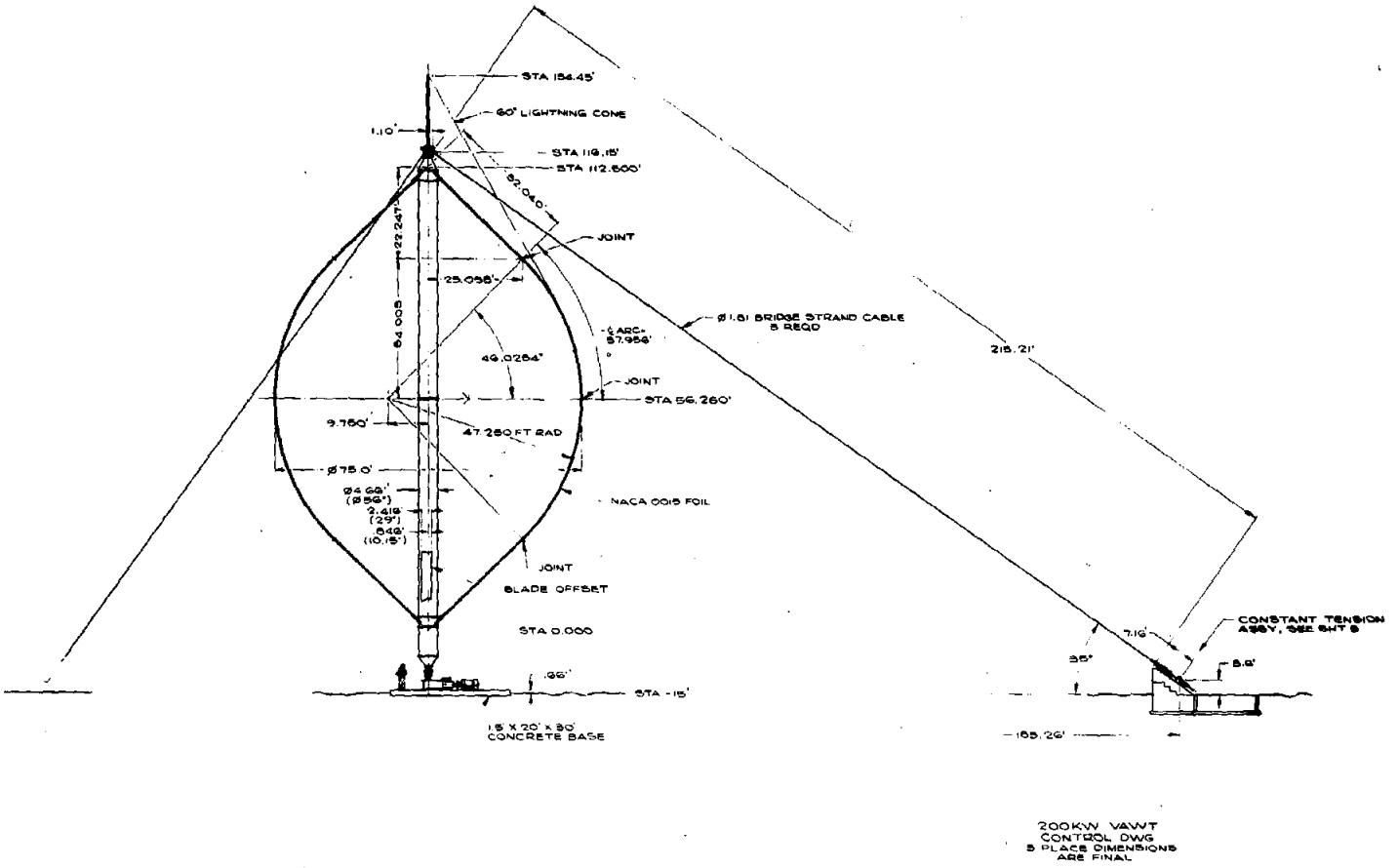

Figure A-1. 200-kW VAWT

LOW SPEED ROTATING PARTS ITEM	MATERIAL	NO REQD	WT-EACH LBS.	WT-TOTAL LBS.	MI SLUG-FT^2
1-UNIVERSAL JOINT ADAPTER TO TRANS	STEEL	1		580	8
2-UNIVERSAL JOINT CROSS	STEEL	1		315	2
3-UNIVERSAL JOINT ADAPTER TO TUBE	STEEL	1		1130	90
4-BOTTOM TUBE EXTENSION	STEEL	1		402	70
5-TUBE	STEEL	2	3087	6174	1078
6-TUBE ADAPTER	STEEL	6	146	876	152
7-TUBE ADAPTER	STEEL	4	182	728	125
8-TOP CONE	STEEL	1		1405	146
9-BEARING	STEEL	1		96	1
10-BLADE	ALUM.	2	2390	4780	107000
11-CLAMP, BLADE, OUTER, LOWER	ALUM.	2	240	480	315
12-CLAMP, BLADE, INNER, LOWER	ALUM.	2	240	480	315
13-CLAMP, BLADE, OUTER, UPPER	ALUM.	2	240	480	315
14-CLAMP, BLADE, INNER, UPPER	ALUM.	2	240	480	315
15-CLAMP ADAPTER	STEEL	4	175	700	306
16-TRANSITION, LOWER	STEEL	2	305	610	68
17-TRANSITION, UPPER	STEEL	2	305	610	68
18-					
19-TUBE, TRANSITION	STEEL	2	596	1192	200
20-JOINT, SLOTTED	ALUM.	6	95	570	14800
				22908 LBS	125374 SLUG FT^2

STATIC AND HIGH SPEED PARTS ITEM	MATERIAL	NO REQD	WT-EACH LBS.	WT-TOTAL LBS.
21-GENERATOR		1		2970
22-BRAKE	STEEL	1		900
23-CLUTCH	STEEL	1		200
24-CALIPERS	STEEL	2	52	104
25-DIFFERENTIAL	STEEL	1		860
26-TRANSMISSION	STEEL	1		5290
27-GUY CABLE ATTACHMENT	STEEL	1		740
28-LIGHTNING PROJECTOR BRUSHOLDER	STEEL	1		22
29-LIGHTNING PROTECTORMAST	STEEL	1		240
30-GUY CABLE SOCKETS	STEEL	6	111	666
31-CABLE	STEEL	3	1473	4419
32-CABLE ATTACHMENT	STEEL	3	390	1170
33-CABLE ATTACHMENT STUD	STEEL	3	184	552
34-CABLE TENSION STUD	STEEL	3	35	105
35-WASHER	STEEL	3	54	162
36-NUT	STEEL	3	130	430
37-WASHER	STEEL	3	8	28
38-WASHER	STEEL	3	3	9
39-NUT	STEEL	3	2	6
40-HYDRAULIC CYLINDER		3		
41-GEARMOTOR	STEEL	3	4	12
				17921 LBS
			TOTAL WEIGHT	40829 LBS

NOTES:

1. BLADE MATERIAL: ALUM ALLOY TENSILE YIELD 35,000 PSI MIN.
2. ALL CARBON STEEL: TENSILE YIELD 30,000 PSI MIN.

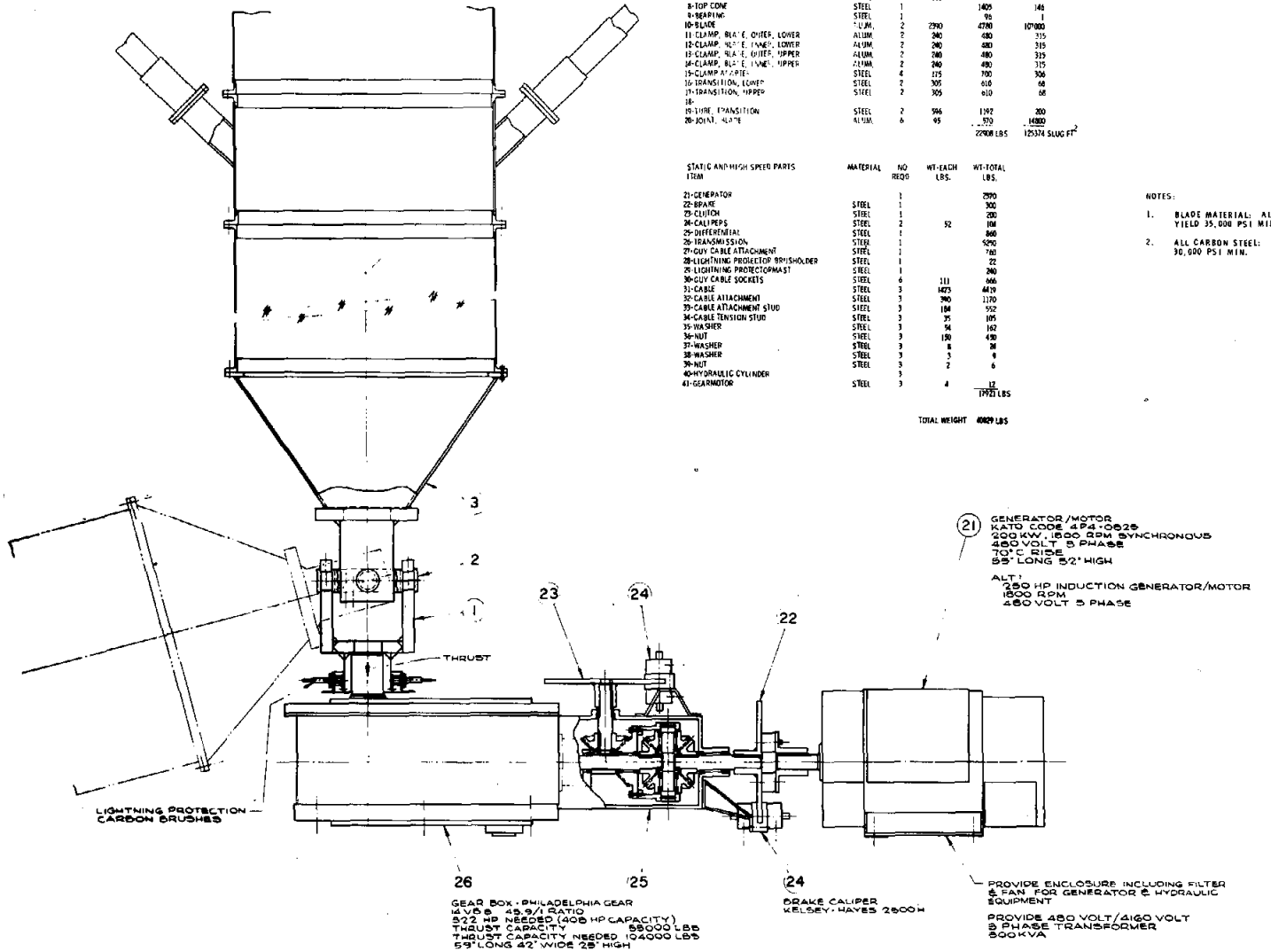

Figure A-2. 200-kW VAWT Differential Hydraulic Clutch

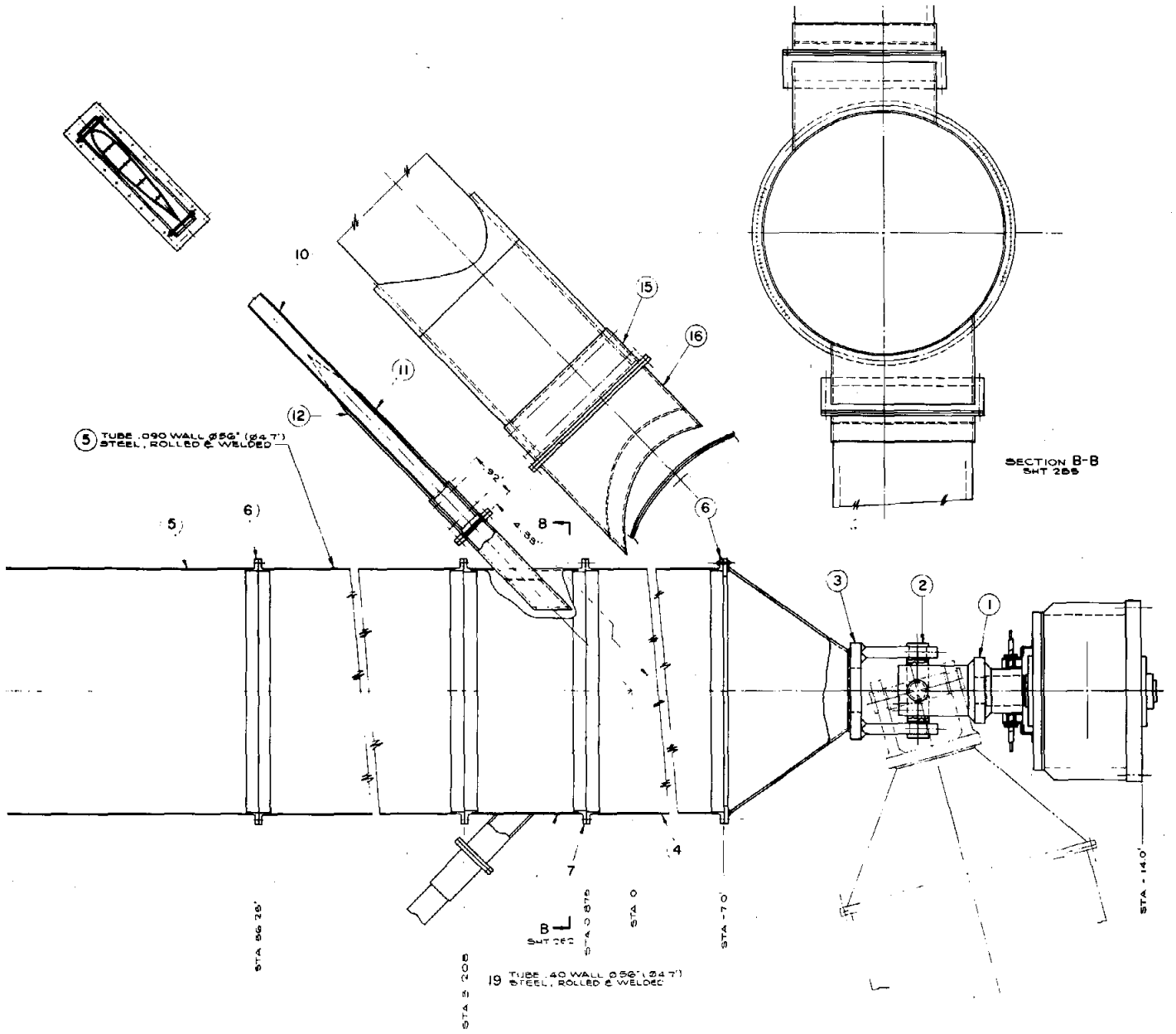

Figure A-3. Blade Adjustment

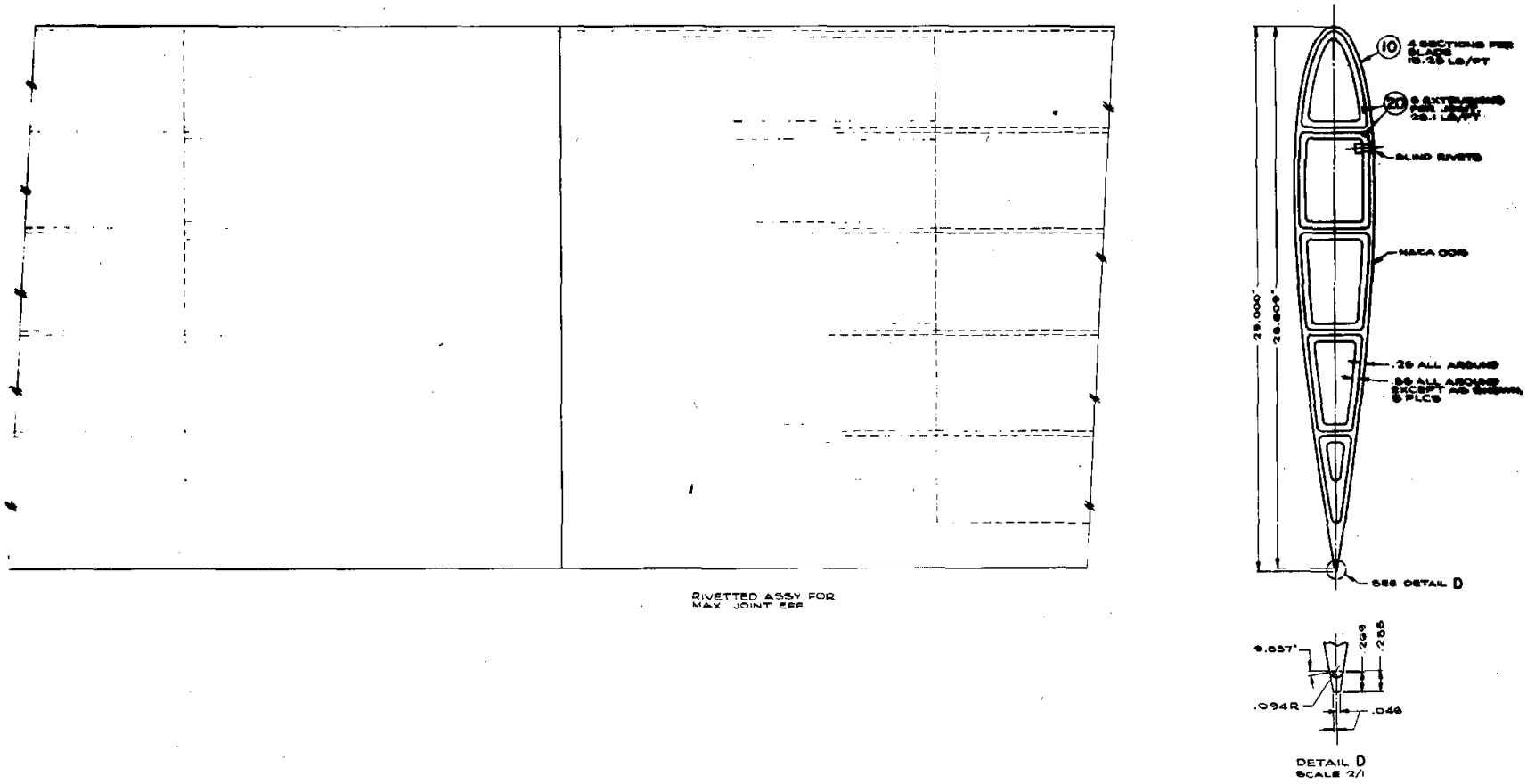

Figure A-4. Blade Joint

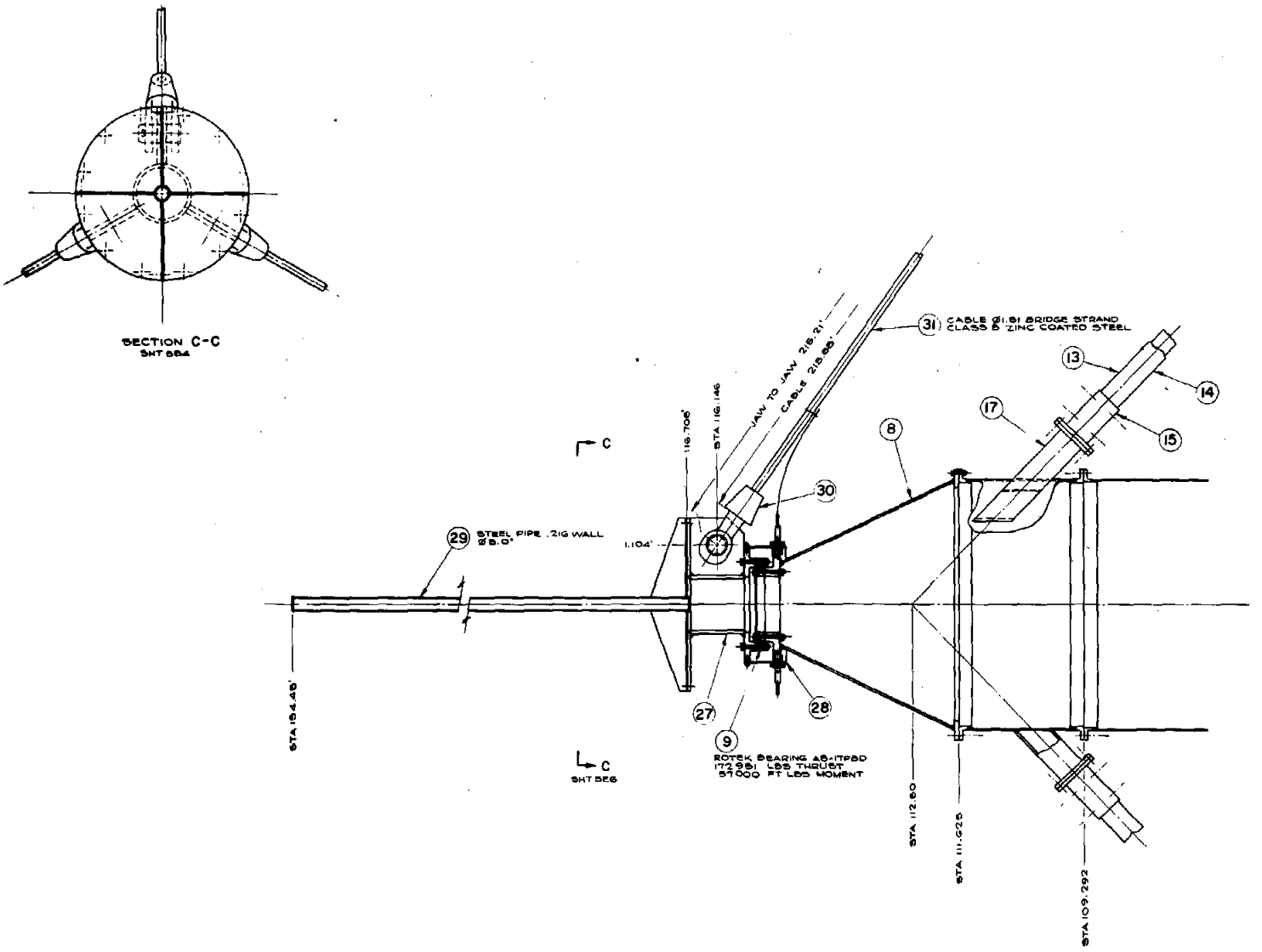

Figure A-5. Guy Cable Attachment

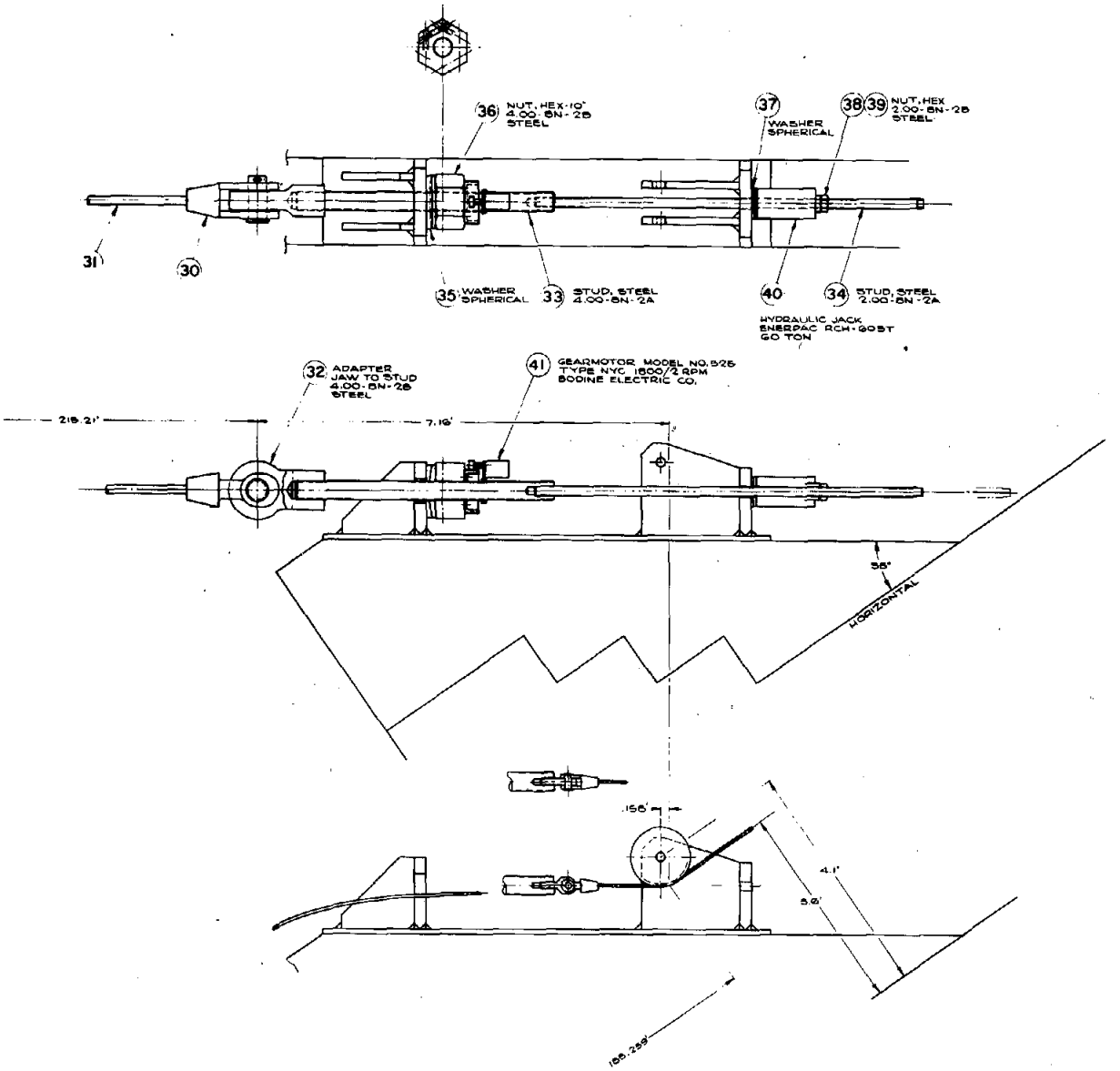

Figure A-6. Guy Cable Adjustment

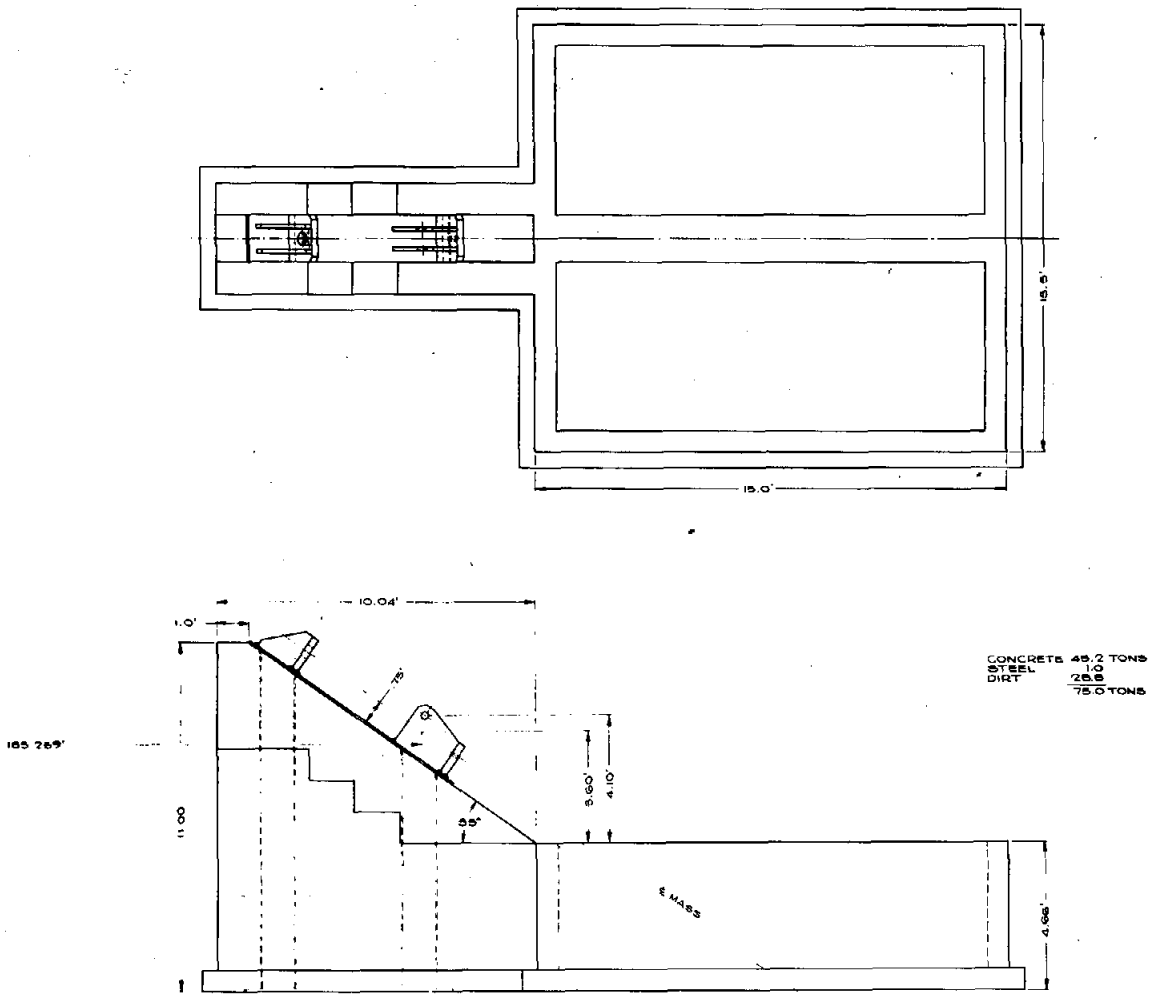

Figure A-7. Guy Cable Anchor

TABLE A-II

Design Features - 500-kW System
(Figures A-8 through A-14)

Actual Rating	Dia. (ft)	H/D Ratio	Steel Tower Dia. (ft)	Steel Tower Wall Thickness (in.)	Steel Tower Weight (lb)	Tiedowns (3) Length (ft)	Tiedowns (3) Cable Area ($in.^2$)	Tiedowns (3) Tiedown Weight (lb)	Blades (2) Chord (in.)	Blades (2) Straight Section Length (ft)	Blades (2) Curved Section Length (ft)	Blades (2) Per-Blade Weight (lb) (incl. joints)
531 kW @ 31 mph, 31.1 rpm	100	1.5	6.3	0.14	17,080	323	3.14	10,620	43	43	98	8136

1st Torsion Freq. (Hz) - 15
1st Bending Freq. (Hz) - 2.6

Pretension - 86,000 lb
1st Tiedown Freq. - 0.77 Hz

Blade Wall Thickness - 0.25 in.
Number of Joints - 3
Total Weight of Joints - 2386 lb

Drive-Train Torques (lb-ft)

Condition	High-Speed Shaft (1800 rpm)	Rotor Shaft (Rotor rpm)	Service Factor	Duty Cycle
Normal Operating	1960	136,000	1.2	3000 h/yr, continuous
Startup	2198	-136,000	1.0	360 starts/yr
Runaway to 36 rpm and Emergency Braking	3380	210,000	1.0	Single use without permanent damage to drive train

System Performance @ 31.1 rpm
(0.076 lbm/ft^3 air density)

Windspeed (mph) At 30 ft Ht	Windspeed (mph) At Turbine Centerline	Turbine Output (kW)	Electrical Output (kW)
8	9.6	2.3	-----
10	12.0	23.2	-----
12	14.4	52.7	.6
14	16.8	91.1	39.0
16	19.2	138.9	86.3
18	21.6	194.1	146.0
20	24.0	253.0	205.9
22	26.4	314.2	267.6
24	28.9	376.3	329.9
26	31.2	437.8	391.1
28	33.6	497.3	450.1
30	36.0	553.3	505.2
31	37.2	579.6	531.0
32	38.4	575.3	526.8
34	40.8	558.1	510.0
36	43.2	542.4	494.5
38	45.6	527.9	480.2
40	48.0	514.5	467.1

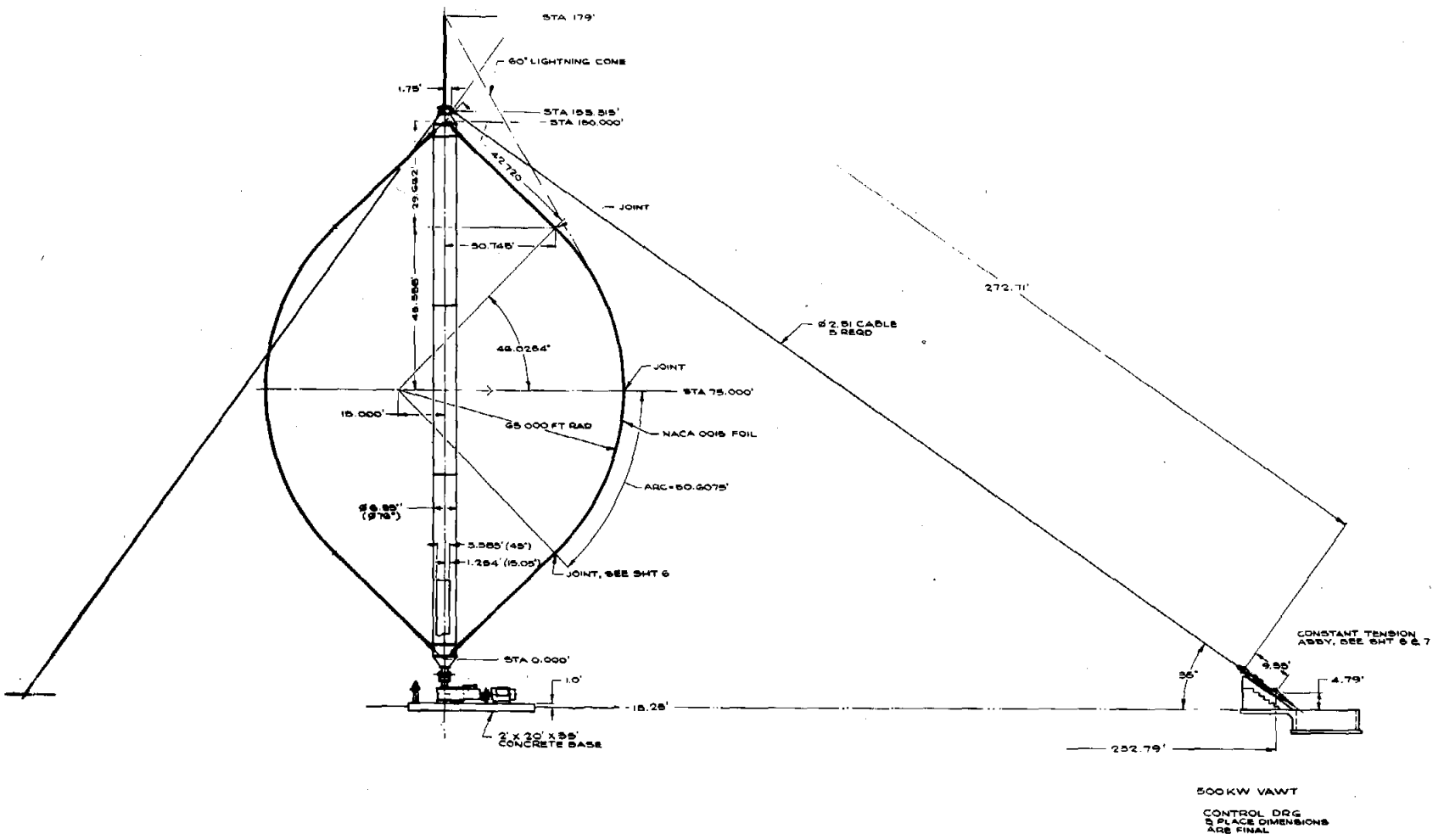

Figure A-8. 500-kW VAWT

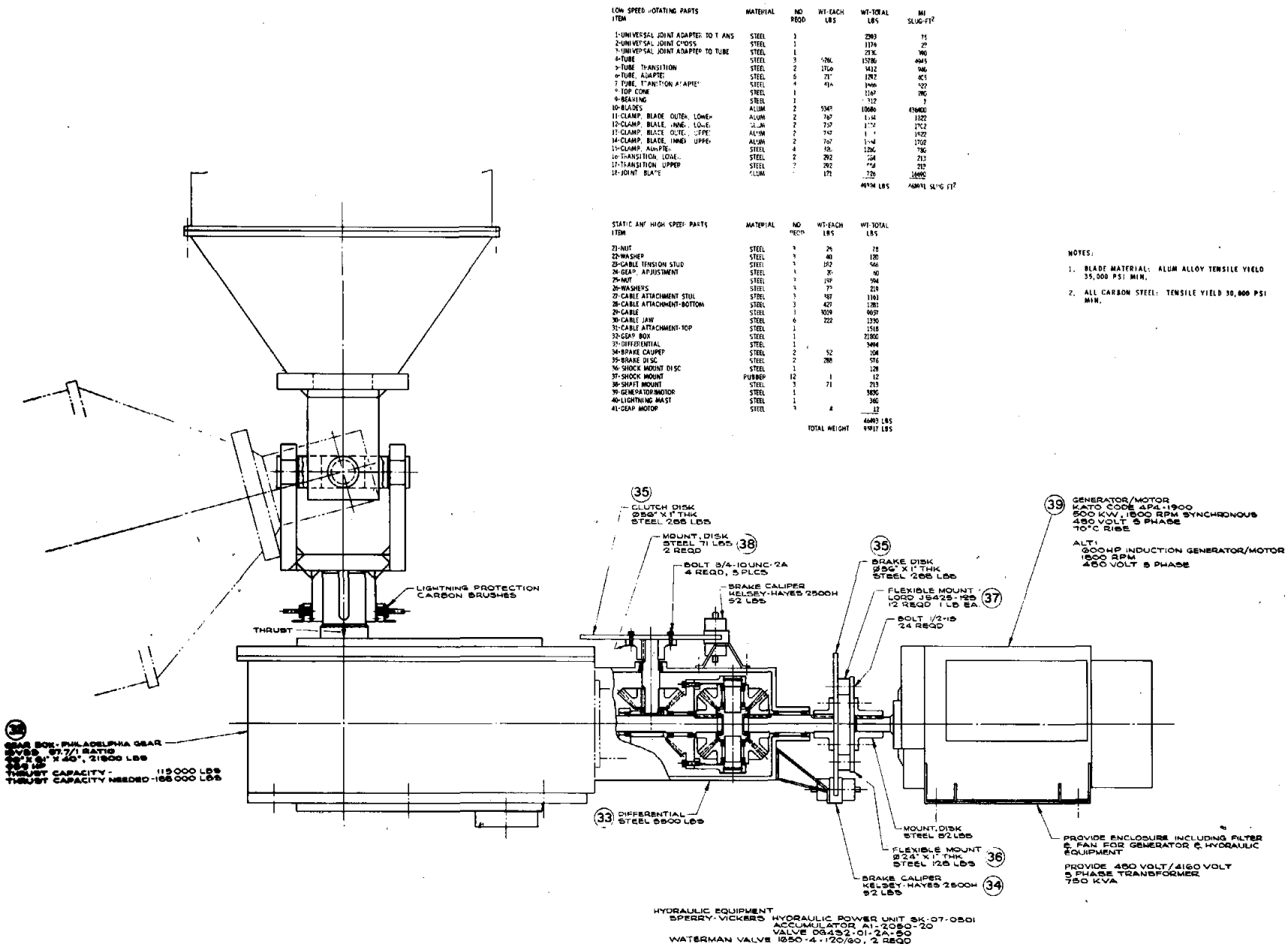

Figure A-9. 500-kW VAWT Differential Hydraulic Clutch

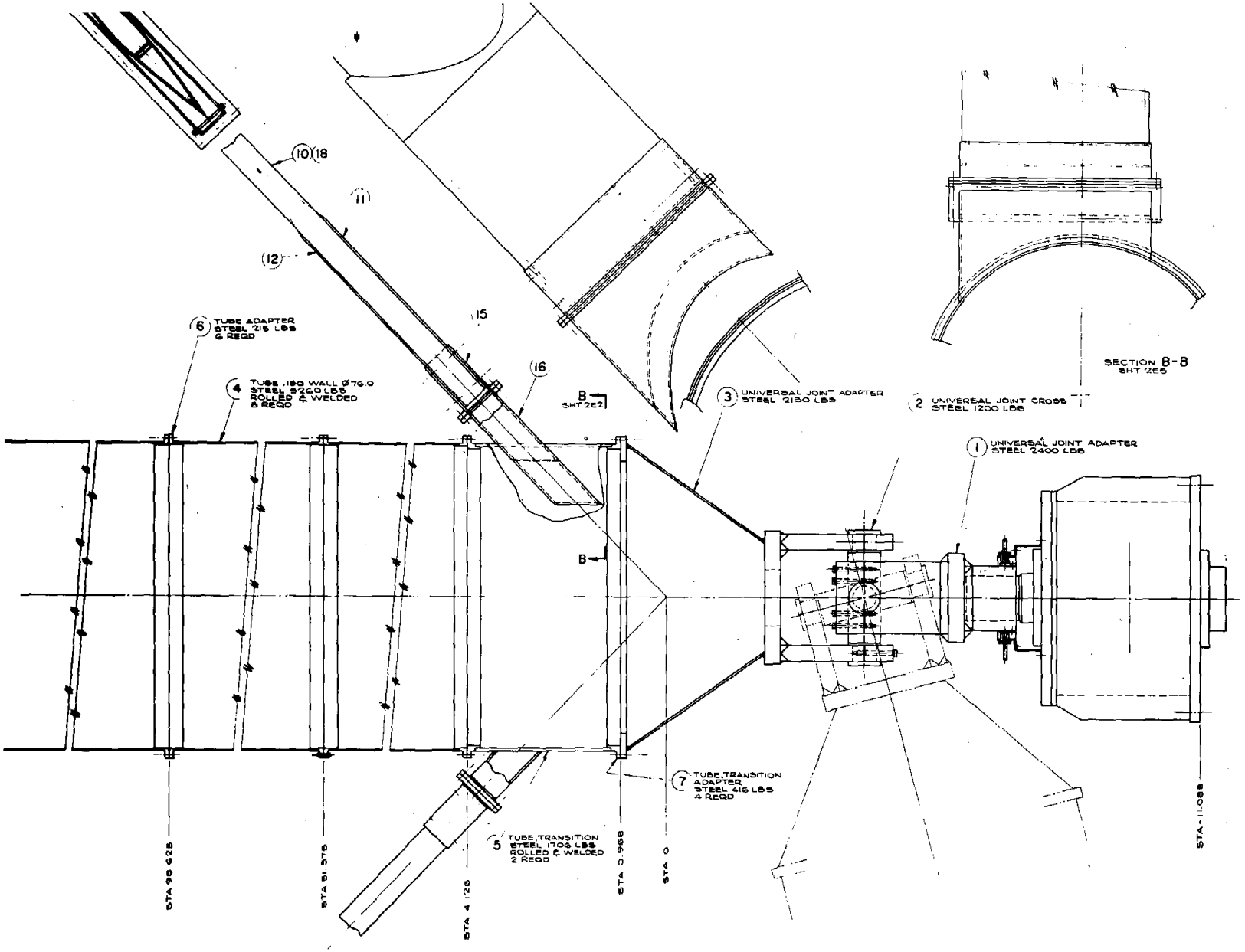

Figure A-10. Blade Attachment

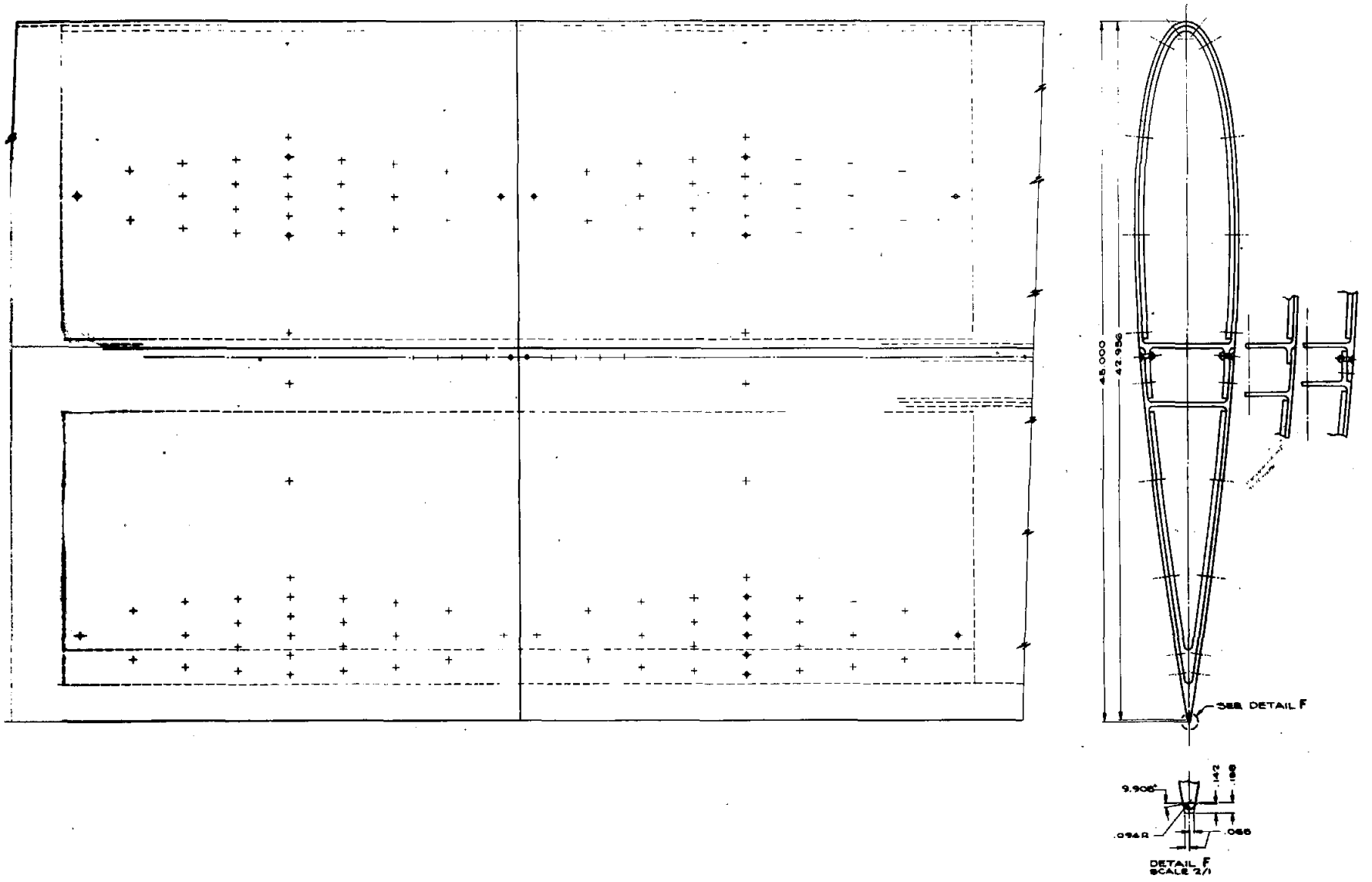

Figure A-11. Blade Joint

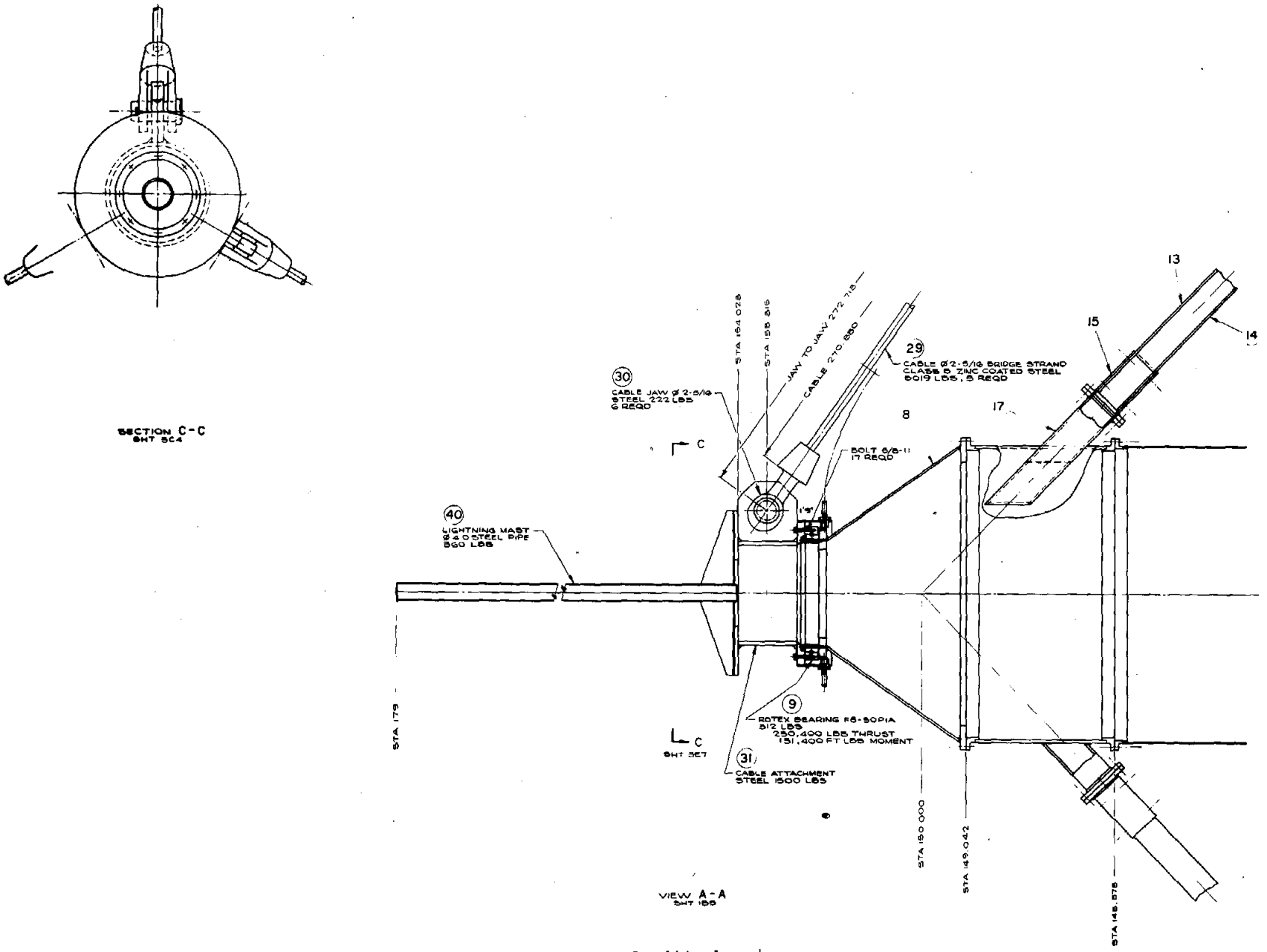

Figure A-12. Guy Cable Attachment

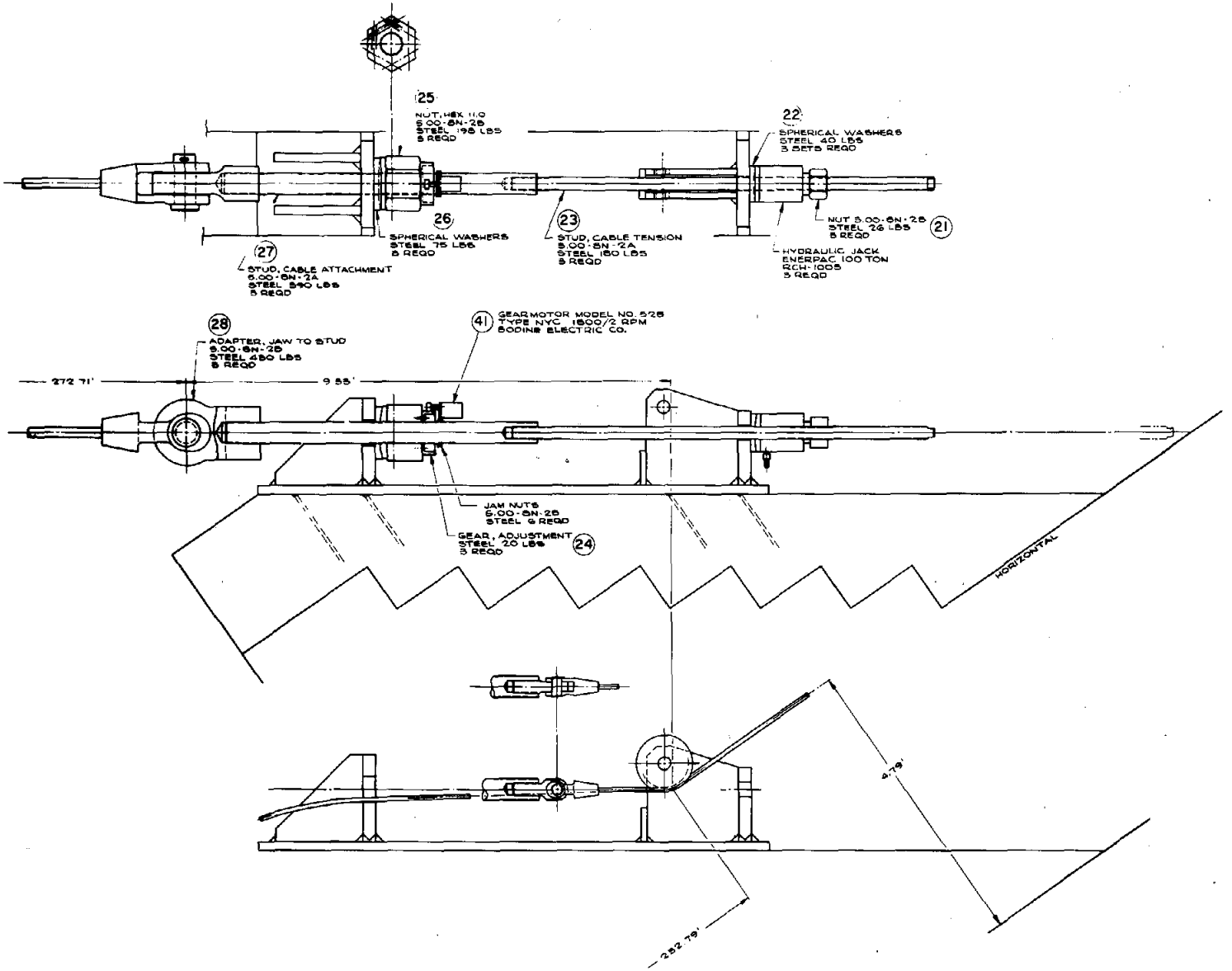

Figure A-13. Guy Cable Adjustment

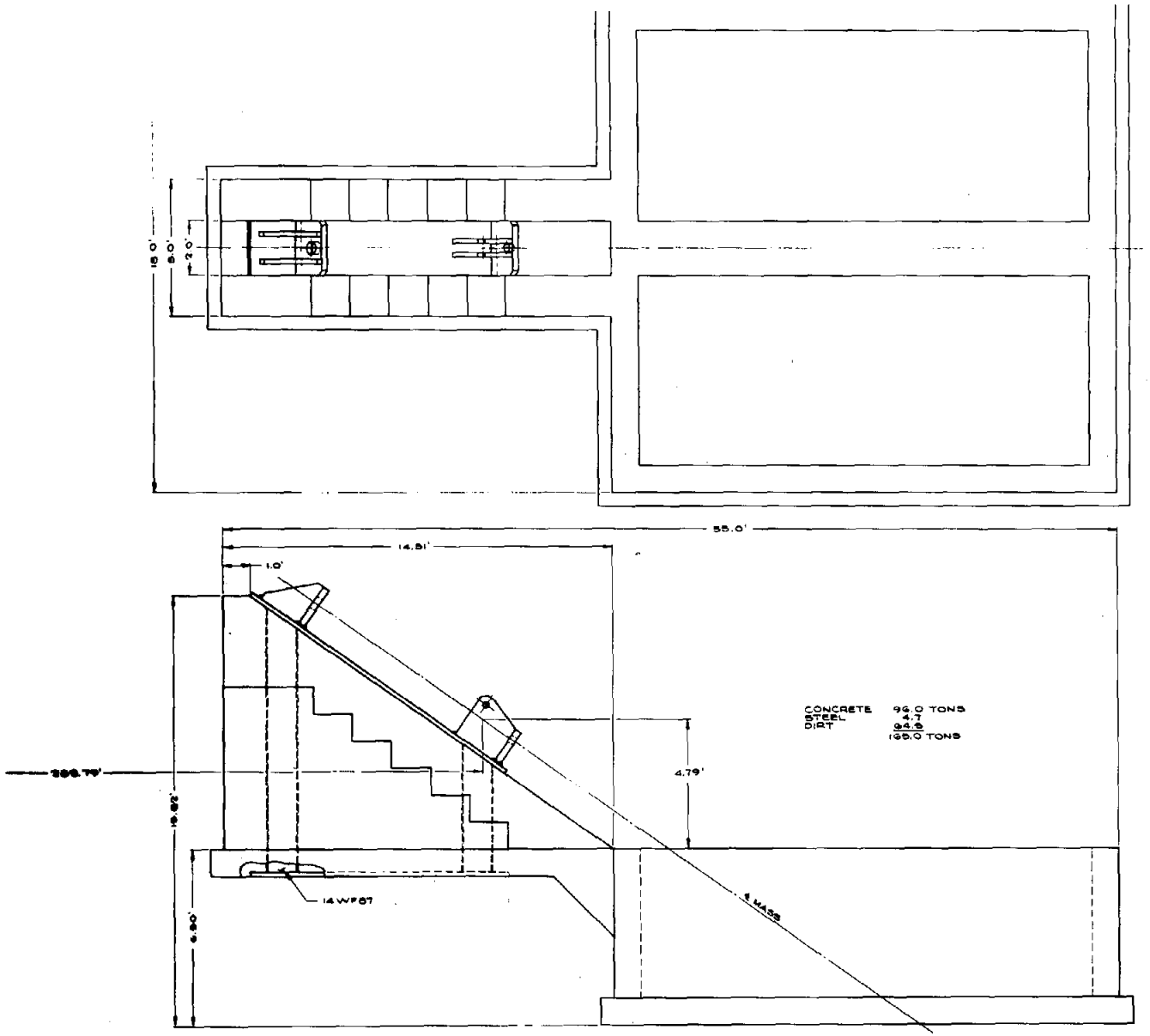

Figure A-14. Guy Cable Anchor

TABLE A-III

Design Features - 1600-kW System
(Figures A-15 through A-22)

Actual Rating	Dia. (ft)	H/D Ratio	Steel Tower Dia. (ft)	Steel Tower Wall Thickness (in.)	Steel Tower Weight (lb)	Tiedowns (3) Length (ft)	Tiedowns (3) Cable Area ($in.^2$)	Tiedowns (3) Tiedown Weight (lb)	Blades (2) Chord (in.)	Blades (2) Straight Section Length (ft)	Blades (2) Curved Section Length (ft)	Blades (2) Per-Blade Weight (lb) (incl. joints)
1330 kW @ 32 mph, 21 rpm	150	1.5	9.4	0.20	102,000	465	6.6	32,100	64.5	64	146.7	36,000

1st Torsion Freq. (Hz) - 10.0
1st Bending Freq. (Hz) - 1.7

Pretension - 230,000 lb
1st Tiedown Freq. - 0.61 Hz

Blade Wall Thickness - 0.38 in.
Number of Joints - 6
Total Weight of Joints - 16,000 lb

Drive-Train Torques (lb-ft)

Condition	High-Speed Shaft (1800 rpm)	Rotor Shaft (Rotor rpm)	Duty Cycle
Normal Operating	5800	497,000	3000 h/yr, continuous
Startup	-5800	-497,000	360 starts/yr
Runaway to 26 rpm and Emergency Braking	11,700	1,000,000	Single use without permanent damage to drive train

System Performance @ 21 rpm
(0.076 lbm/ft^3 air density)

Windspeed (mph) At 30 ft Ht	Windspeed (mph) At Turbine Centerline	Turbine Output (kW)	Electrical Output (kW)
8	10.3	14.7	------
10	12.8	71.2	------
12	15.4	150.3	28.4
14	18.0	252.9	130.7
16	20.5	379.1	256.0
18	23.1	519.1	439.1
20	25.6	666.8	600.7
22	28.2	818.1	765.6
24	30.8	969.4	929.2
26	33.3	1116.5	1087.8
28	35.9	1255.8	1237.0
30	38.5	1342.8	1330.0
32	41.0	1300.2	1284.6
34	43.6	1261.4	1243.0
36	46.2	1225.8	1205.1
38	48.7	1193.1	1170.0
40	51.3	1162.9	1137.6

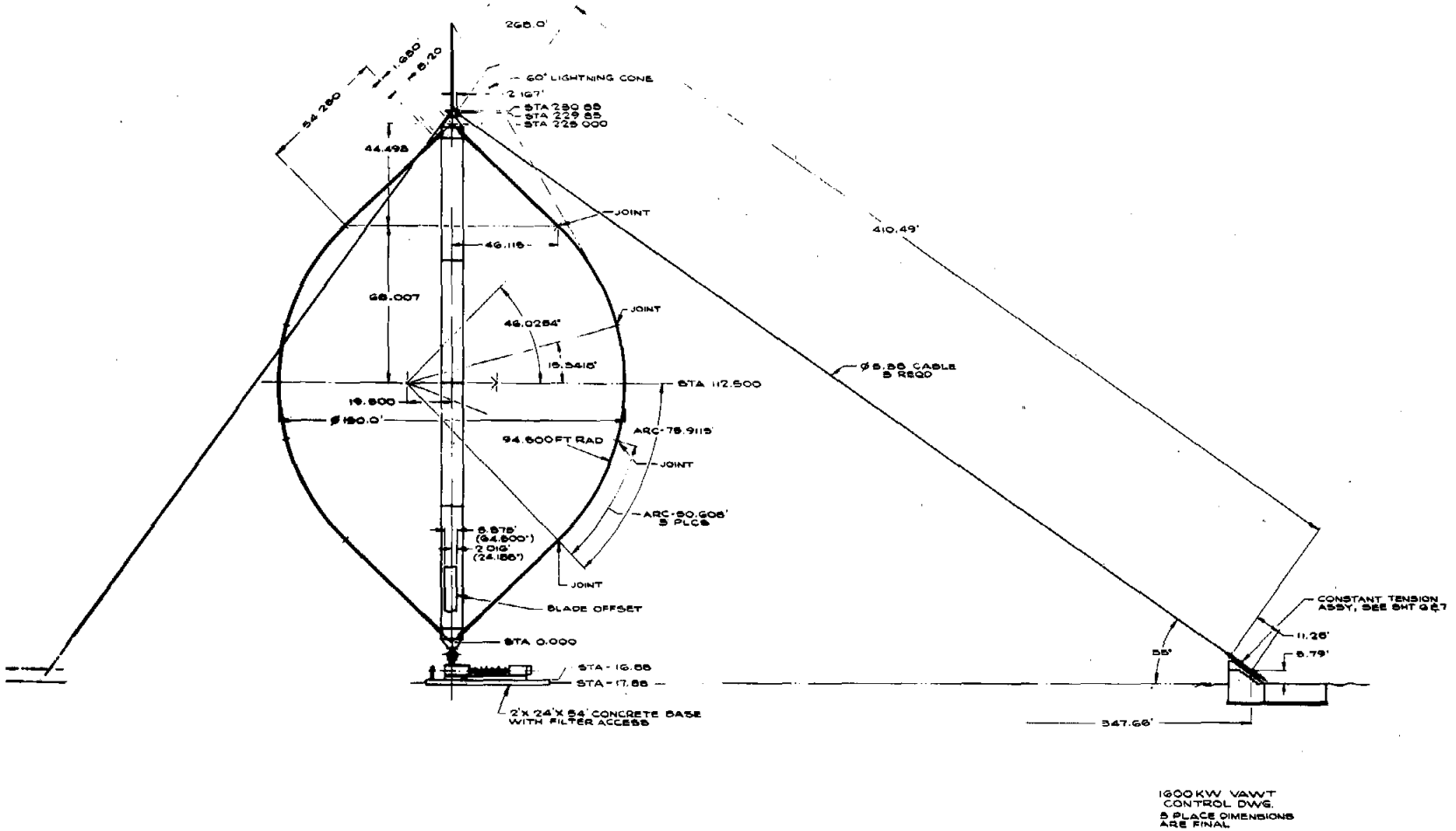

Figure A-15. 1600-kW VAWT

LOW SPEED ROTATING PARTS ITEM	MATERIAL	NO. REQD	WT EACH LBS	WT TOTAL LBS	MI SLUG-FT^2
1-UNIVERSAL JOINT ADAPTER TO TRANS	STEEL	1		7290	369
2-UNIVERSAL JOINT CROSS	STEEL	1		3417	134
3-UNIVERSAL JOINT ADAPTER TO TUBE	STEEL	1		12796	3515
4-TUBE	STEEL	4	12651	50605	38810
5-TUBE, TRANSITION	STEEL	2	6672	13342	6396
6-TUBE ADAPTER	STEEL	8	363	2672	4633
7-TUBE TRANSITION ADAPTER	STEEL	4	1321	5283	3531
8-TOP CONE	STEEL	1		6700	2920
9-BEARING	STEEL	1		484	12
10-BLADES	ALUM	2	19470	38940	3481859
11-CLAMP, BLADE, OUTER, LOWER	ALUM	2	1980	3920	1148a
12-CLAMP, BLADE, INNER, LOWER	ALUM	2	1980	3920	10862
13-CLAMP, BLADE, OUTER, UPPER	ALUM	2	1980	3920	1148a
14-CLAMP, BLADE, INNER, UPPER	ALUM	2	1980	3920	10862
15-CLAMP, ADAPTER	STEEL	4	1006	4024	5314
16-TRANSITION, LOWER	STEEL	2	1275	2550	2200
17-TRANSITION, UPPER	STEEL	2	1275	2550	2200
18-JOINT, BLADE	ALUM	8	746	5966	626784
				172101 LBS	4229133 SLUG-FT^2

STATIC & HIGH SPEED PARTS ITEM	MATERIAL	NO. REQD	WT. EACH LBS.	WT. TOTAL LBS.
20-FLEXIBLE COUPLING	STEEL	8	175	1050
21-CLUTCH DISC	STEEL	2	473	946
22-CLUTCH SHAFT	STEEL	1		183
23-CLUTCH SHAFT	STEEL	1		200
24-CLUTCH CONE	STEEL	2	272	544
25-BRAKE DISC	STEEL	2	542	1084
26-BRAKE SHAFT	STEEL	1		417
27-BRAKE PAD HOLDER	STEEL	4	26	104
28-ARM, BRAKE PAD	STEEL	4	12	48
29-POST, BRAKE ARM	STEEL	2	25	50
30-HOLDER, BRAKE BEARING	STEEL	2	205	410
31-HOLDER, CLUTCH BEARING	STEEL	2	213	426
32-BEARING, RADIAL	STEEL	2	23	46
33-BEARING, RADIAL	STEEL	4	9	36
34-BEARING, THRUST	STEEL	2	5	10
35-THRUST PLATE	STEEL	1		44
36-CYLINDER, HYDRAULIC	STEEL	5	3	15
37-CLEVIS EYE, MOUNTING	STEEL	4	.5	2
38-BKT., HYDRAUL. CYLINDER	STEEL	2	40	80
39-GUY CABLE ATTACHMENT	STEEL	1		6334
40-LIGHTNING MAST	STEEL	1		1081
41-LIGHTNING RING, LOWER	BRASS	1		47
42-LIGHTNING RING, UPPER	BRASS	1		57
43-GEARBOX	STEEL	1		46000
44-GUY CABLE SOCKETS	STEEL	6	584	3504
45-CABLE, BRIDGE STRAND	STEEL	3	9764	29292
46-FLEXIBLE COUPLING	RUBBER	45	1	45
47-GENERATOR, MOTOR	STEEL	1		10400
48-AUP, SOCKET TO STUD	STEEL	37	1095	3015
49-STUD, CABLE ATTACHMENT	STEEL	3	692	2076
50-WASHER, SPHERICAL	STEEL	3	19	57
51-NUT, HEX	STEEL	3	212	636
52-GEAR, ADJUSTMENT	STEEL	3	32	96
53-GEARMOTOR	STEEL	3	10	30
54-WASHER, SPHERICAL	STEEL	3	27	81
55-HYDRAULIC JAC	STEEL	3	5901	1770
56-NUT, HEX	STEEL	3	29	87
57-STUD, CABLE TENSION	STEEL	3	462	1386
				113809 LBS
		TOTAL WEIGHT		280910 LBS

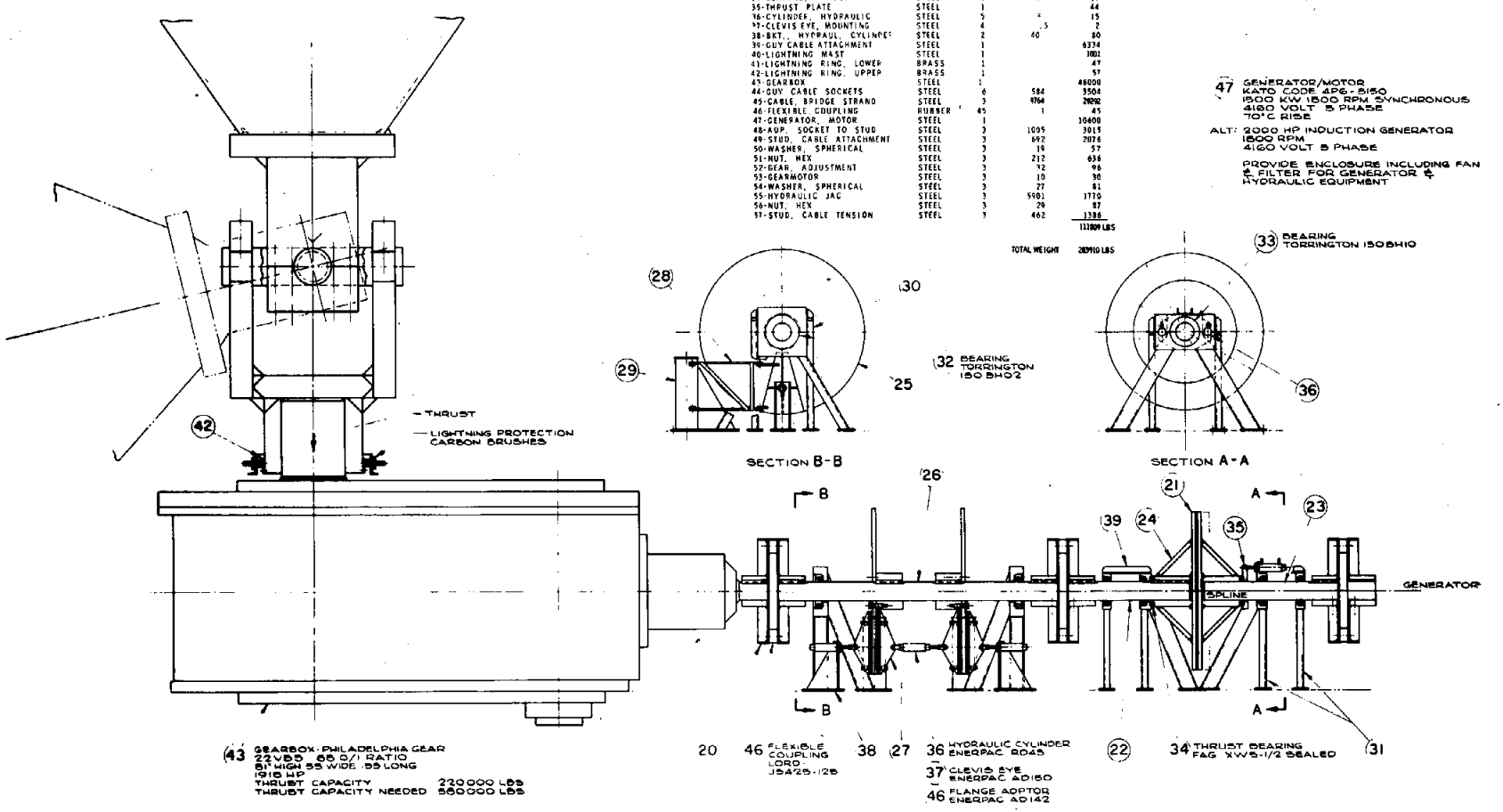

Figure A-16. 1600-kW VAWT, Hydraulic Clutch

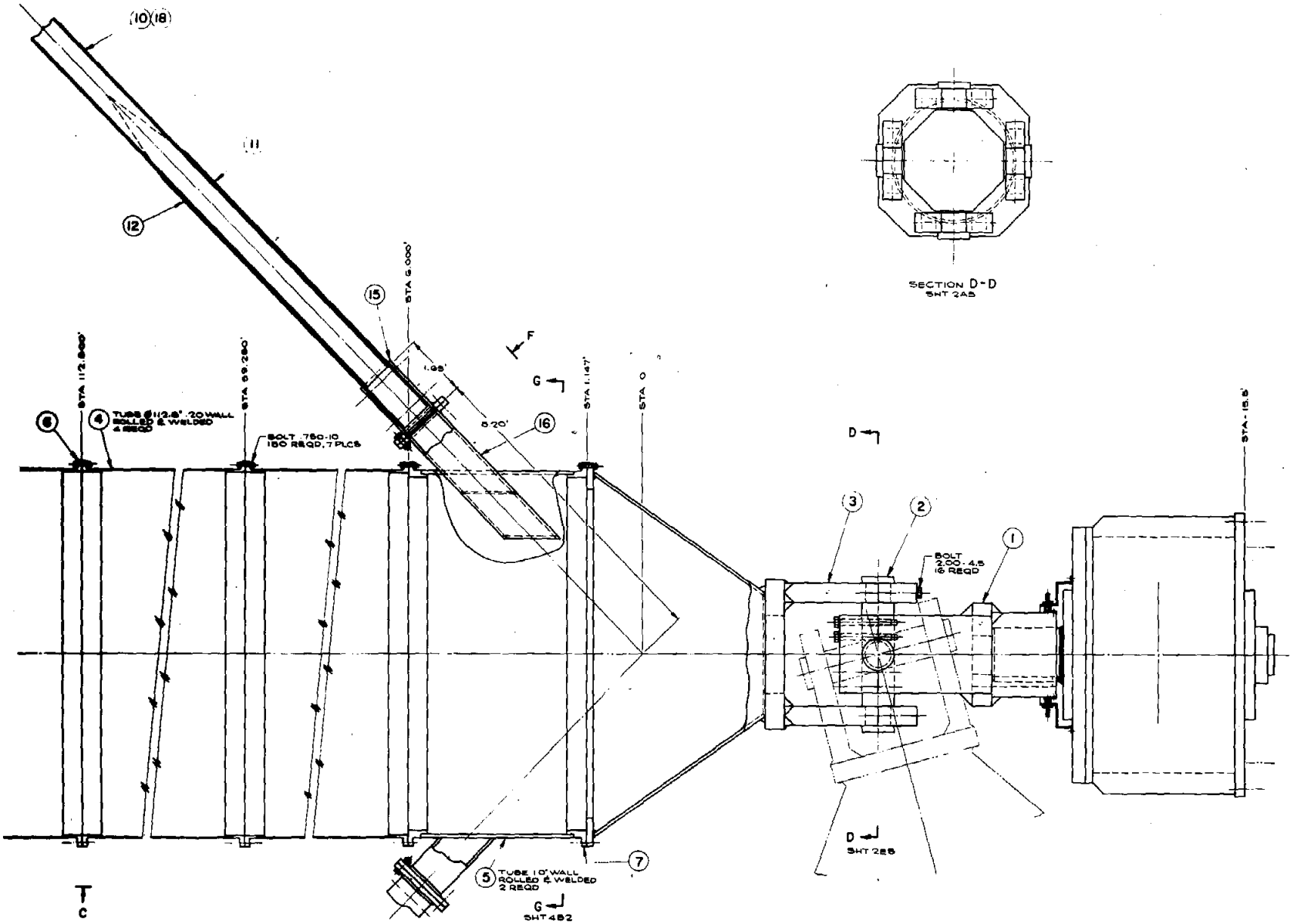

Figure A-17. Blade Attachment

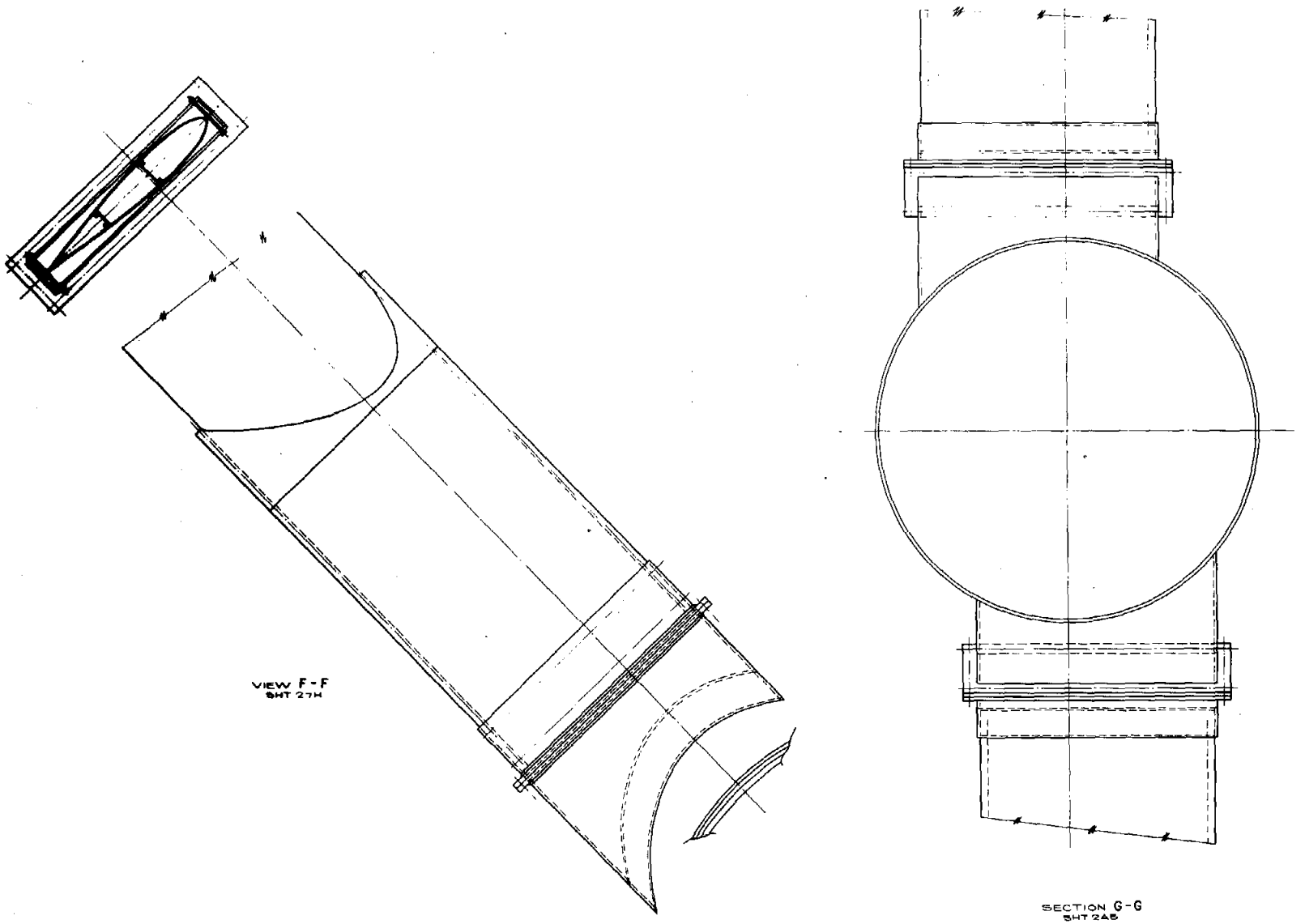

Figure A-18. Blade Attachment

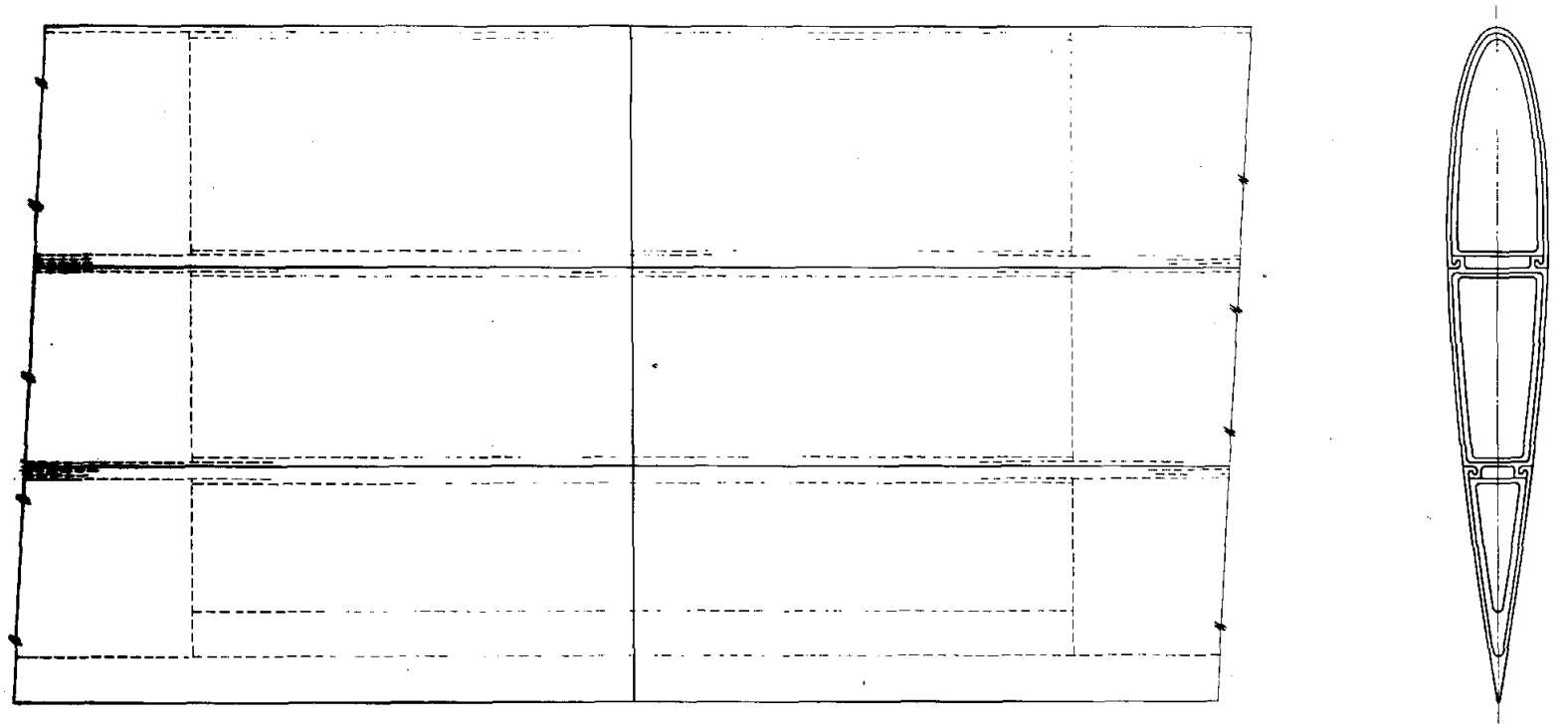

Figure A-19. Blade Joint

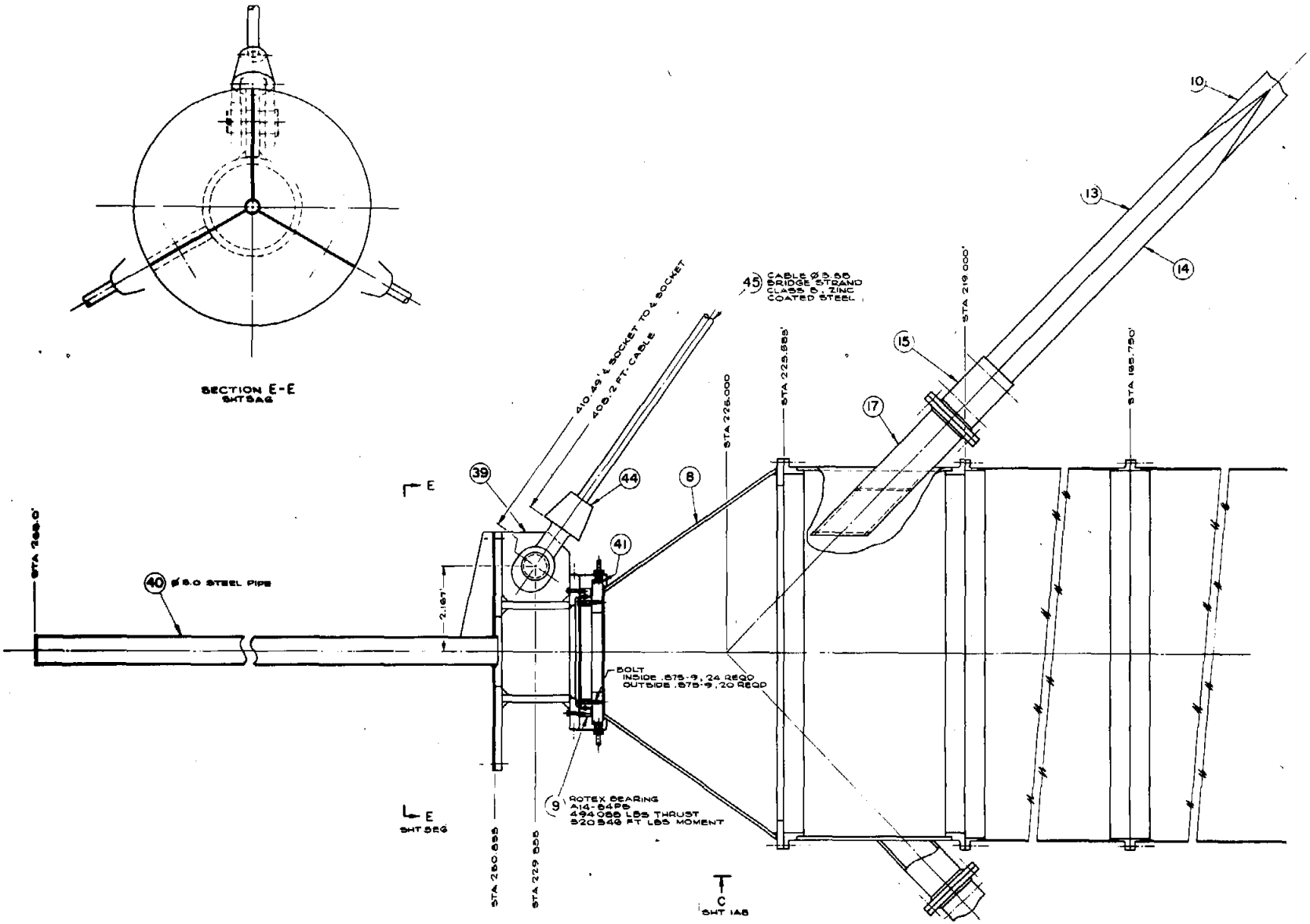

Figure A-20. Guy Cable Attachment

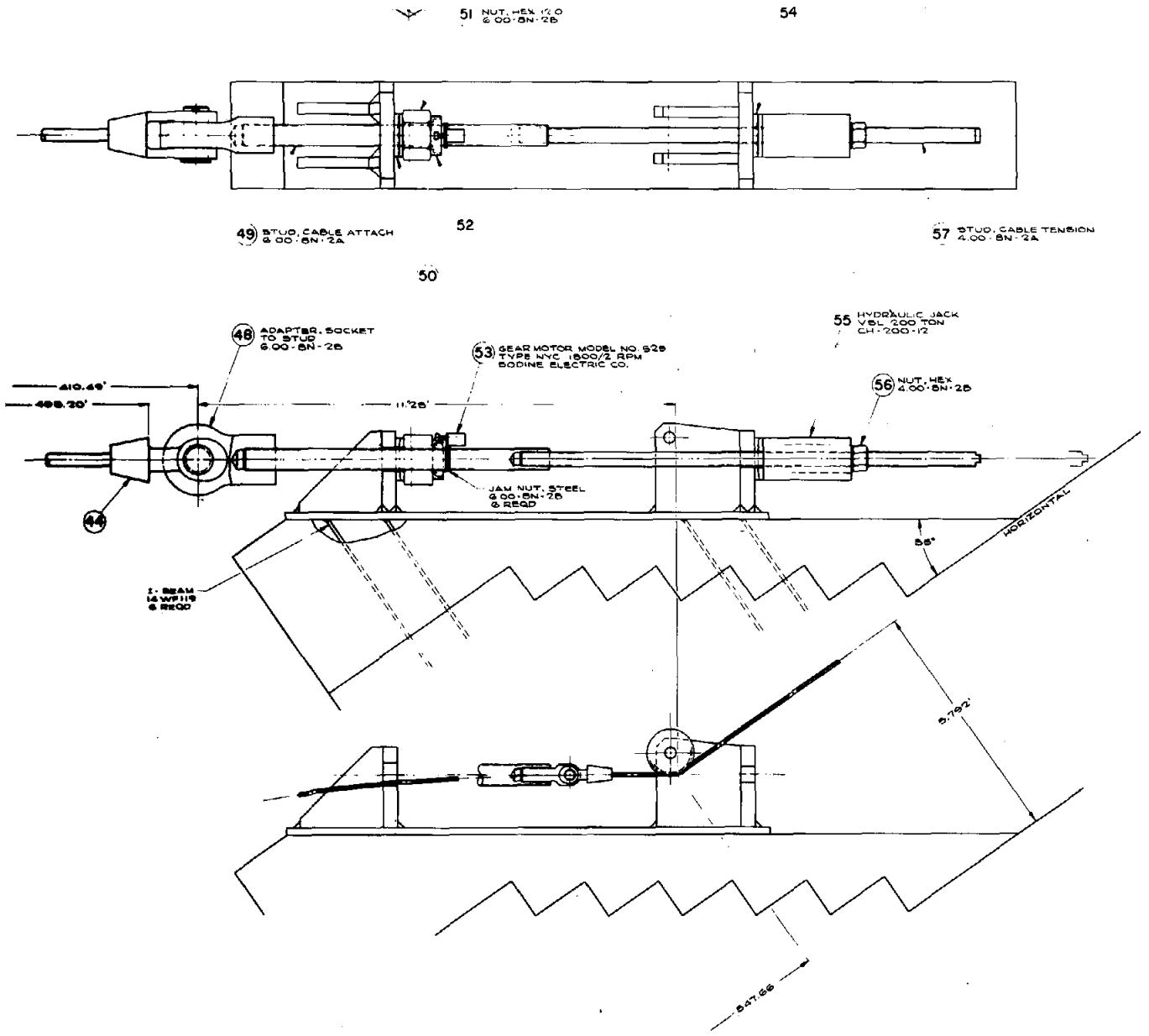

Figure A-21. Guy Cable Adjustment

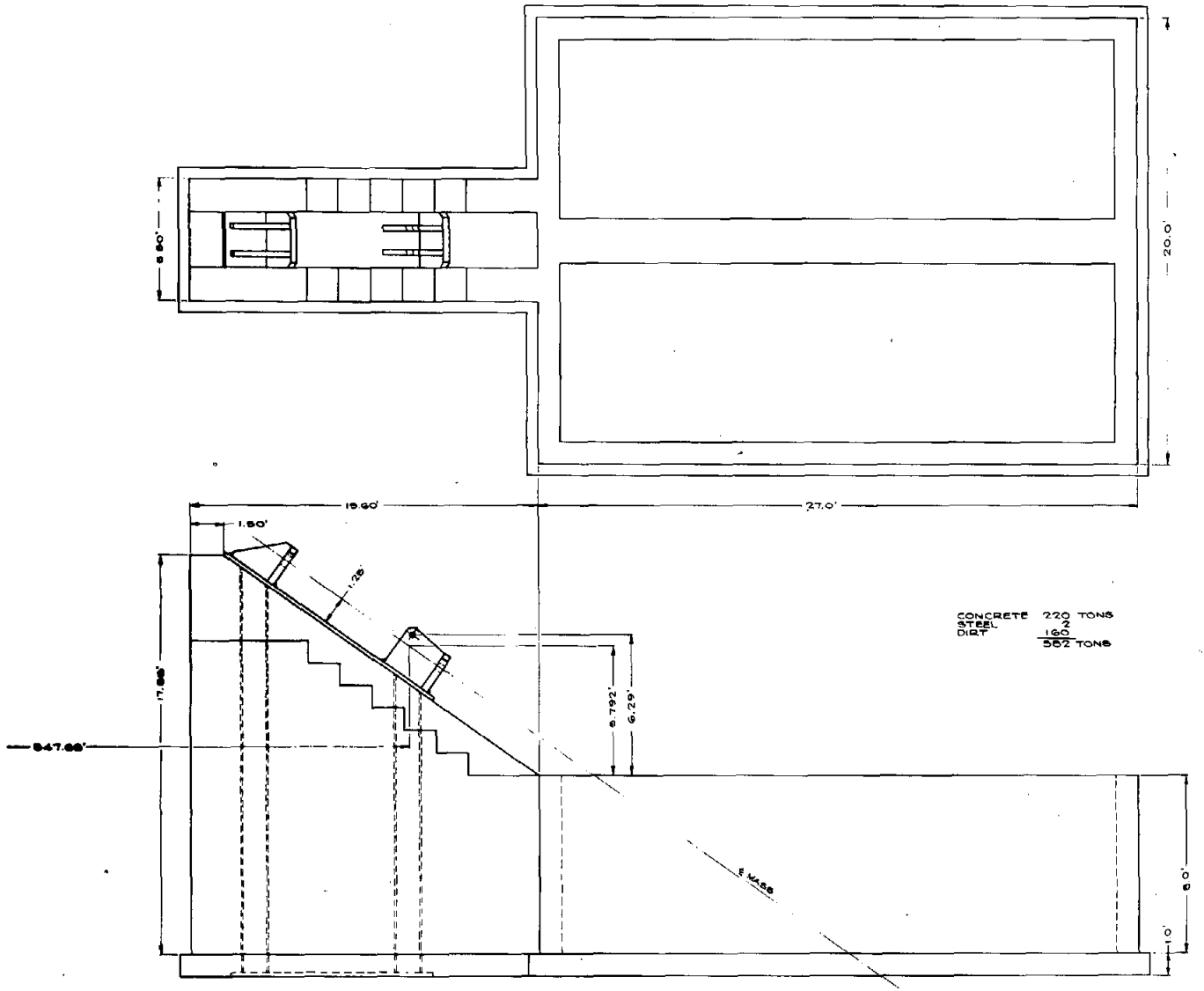

Figure A-22. Guy Cable Anchor

TABLE A-IV

Rotor Geometry for the Point Designs

Nominal Rating (kW)	10	30	120	200	500	1600
Diameter x Height (ft)	18 x 27	30 x 45	55 x 83	75 x 120	100 x 150	150 x 225
Collection Area (ft^2)	324	900	3000	5600	10,000	22,500
Ground Clearance (ft)	10.	10.	10.	17.	13.	17.
Blade Chord (in.)	6	11	24	29	43	64
Blade Wall Thickness (in.)	.125	.22	.24	.25	.25	.38
Rotor Solidity	.104	.120	.135	.120	.134	.134
Tower Diameter (ft)	2.0	2.4	3.7	4.7	6.3	9.4
Tower Wall Thickness (in.)	.032	.032	.060	.090	.140	.20
Tiedown Tension (lb)	1700	5000	20,000	46,000	86,000	230,000
Number of Blades	2	2	2	2	2	2

TABLE A-V

Performance Characteristics of the Point Designs
(15-mph Median Distribution)*

Nominal Rating (kW)	10	30	120	200	500	1600
Actual Peak Output (kW)	8	26	116	226	531	1330
Rated Windspeed (mph), 30-ft Reference	34	32	31	30	31	30
Annual Energy Collection (MWh/yr)	13.7	51.6	246	490	1070	2950
Plant Factor (%)	19.3	22.3	24.0	24.4	22.6	24.9
Rated Rotor Torque (ft-lb)	398	2260	17,600	45,200	136,000	497,000
Rotor rpm	163	95.0	52.0	40.1	31.1	21.0
Blade Reynolds Number (Millions)	.47	.89	1.8	2.3	3.6	5.5
Maximum Power Coefficient	.34	.37	.38	.37	.39	.39

*All results are for sea-level air density. Performance calculations are from Version 16 of the optimization model.

TABLE A-VI

Predicted Component Weights (lb) for the Point Designs

Nominal Rating (kW)	10	30	120	200	500	1600
Weights (lb):						
Blades	138	857	3640	6630	16,300	72,600
Tower	368	1050	4890	13,900	27,400	101,000
Tiedowns	105	353	1710	4680	9300	31,400
Transmission	48	272	2110	5430	16,300	59,600
Generator	161	434	1420	2420	4800	9990
Total	819	2970	13,800	33,000	74,000	275,000
Annual kWh per Pound of System Weight (kWh/lb)	16.4	17.2	17.7	14.6	14.1	10.6

TABLE A-VII

Predicted Component Costs for the Point Designs*

Nominal Rating (kW)	10	30	120	200	500	1600
	Component Costs ($)					
Blades	1180	3110	9120	21,300	47,200	160,000
Tower	635	1910	8260	22,500	46,500	176,000
Tiedowns	262	883	4290	11,700	23,800	78,500
Transmission	399	1570	8020	17,200	41,200	116,000
Generator and Controls	2650 (460 V)	3920 (460 V)	9180 (460 V)	22,600 (4160 V)	45,300 (4160 V)	67,300 (4160 V)
Field Erection and Foundations	1260	4630	15,100	26,400	44,300	119,000
Total	6380	16,000	54,000	122,000	248,000	717,000
$/kWh @ 15% Annual Charge	6.97	4.65	3.30	3.72	3.50	3.65

*All costs are from Version 16 of the optimization model.

APPENDIX B

Clutch and Brake Design Calculations

APPENDIX B

Clutch and Brake Design Calculations for 120 kW VAWT

Clutch

A VAWT cannot be started by the wind; it must be started by an outside source such as a motor. The generator can be used as a starting motor if the motor is allowed to operate at full speed during startup. This is done by running the motor at full speed and using a clutch to engage and start the VAWT. While producing the rated torque, the clutch is allowed to slip until the VAWT is up to rated speed. This prevents motor and drive-train overload as might be experienced if the VAWT were connected directly to the motor during motor start.

The electric motor is started, brought up to full speed, and synchronized with the grid in the case of a synchronous motor. The clutch, which is engaged by a hydraulic cylinder, slips until the VAWT is brought up to rated speed with the clutch providing rated torque.

The amount of energy required to start the VAWT is the energy converted into VAWT kinetic energy plus the energy converted into heat in the clutch disk owing to slippage of the clutch pads upon the clutch plate. The kinetic energy of the VAWT is given by the equation

$$U = \frac{I\omega^2}{2} \tag{B1}$$

where

U = kinetic energy (ft-lb)

I = VAWT moment of inertia (slug/ft^2)

ω = angular velocity (rad/s)

The amount of energy converted into VAWT kinetic energy is ~ 571,000 ft-lb. The angular acceleration of the VAWT by using rated torque is given by

$$\gamma = \frac{T}{I} \tag{B2}$$

where

γ = angular acceleration (rad/s^2)

T = rated torque (lb-ft)

I = moment of inertia (slug/ft^2)

The starting time under these conditions is given by

$$t = \frac{\omega}{\gamma} \tag{B3}$$

where

t = time (s)

With the rated VAWT torque of 17,600 lb-ft and the VAWT moment of inertia of 38,210 slug/ft^2, the VAWT acceleration is 0.461 rad/s^2 and the starting time is 11.87 seconds. With the motor providing rated torque to the clutch for 11.87, the starting energy requirement is given by

$$U_s = \frac{T(RPM)}{5252} \times 550 \times t \quad \text{ft-lb} \tag{B4}$$

where

U_s = starting energy (ft-lb)
T = torque (lb-ft)
RPM = turbine rpm
t = time (s)

Torque differs from the low-speed side of the transmission to the high-speed side by the transmission gear ratio. The energy calculations were done by using the torque on the low-speed side of the transmission. The amount of energy to be absorbed in the brake and clutch is the same on either side of the transmission although the torques differ by the transmission gear ratio.

The starting energy requirement is 1.142×10^6 ft-lb, of which 571,000 ft-lb are converted to VAWT inertia and 571,000 ft-lb or 734 Btu are converted to heat in the clutch plate A 1-in.-thick steel plate is selected as the clutch to conform with the plate heat-flow theory of putting heat into one side of an infinitely thick plate. The plate is not infinitely thick, but is considered as such for the short time considered.[5] The only thing considered here is the one-time startup of the VAWT without a wind. The number of starts, the wind velocity, the clutch-plate temperature, and the frequency of starts change only the size of the clutch, but not its design principles. Clutch-plate temperatures are given as follows

$$\theta = \theta_s - (\theta_s - \theta_o)\, f_1\left(\frac{x}{\sqrt{\alpha t}}\right) °F. \tag{B5}$$

where

θ = temperature, at distance x from heated surface (°F)

θ_s = heated surface temperature (°F)

θ_o = starting temperature (°F)

x = distance from heated surface (ft)

t = time (h)

α = thermal diffusivity (ft^2/h)

$$\alpha = \frac{K}{\rho C}$$

where

K = coefficient of thermal conductivity ($Btu/h \cdot ft^2 \cdot °F/ft$ = 23.5 for 1025 steel[3])

C = specific heat ($Btu/lb°F$ = 0.126)

ρ = density (lb/ft^3)

During startup it is assumed that the maximum clutch-plate starting and surface temperatures are 100°F and 400°F, respectively. With these assumptions derived from Eq. (B5) and Fig. B1 (Ref. 5), the temperature $\frac{1}{2}$ in. from the heated surface of the

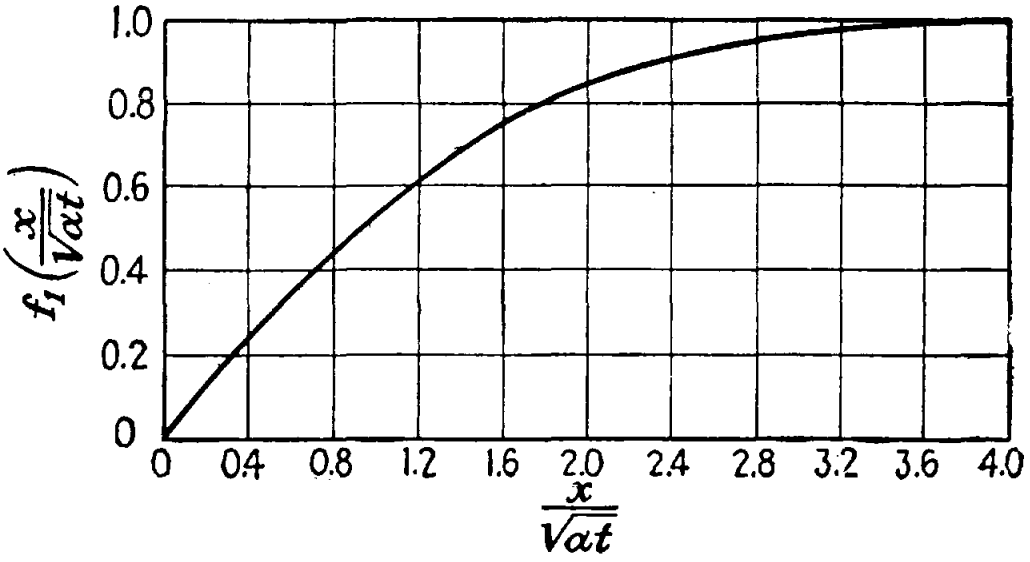

Figure B1. Clutch Temperature Function f_1*

clutch plate is found to be 180°F and the temperature 1 in. from the heated surface is 120°F. This permits an energy absorption of the clutch plate of 732 Btu/ft^2 during startup.

*Reprinted by permission of McGraw-Hill Book Company from p. 195 of Ref. 5.

With a required energy absorption of 734 Btu, an area of 1 ft^2 is needed to start the turbine. With a coefficient of friction between the clutch pad and the clutch disk of 0.24 and an average radius of 5 in., a hydraulic cylinder force of 4800 lb is required to start the VAWT at the rated torque of 480 lb-ft.

Brake

The brake disk is designed by the same method as the clutch. The amount of energy that must be absorbed to stop the turbine is determined and the brake area can be calculated. Table III shows that runaway torque due to wind is 30,400 lb-ft at a turbine speed of 63 rpm. Inertial energy of the turbine at 63 rpm is 832,000 ft-lb; the energy due to the wind during stopping is determined by the selected stopping torque of the brake upon the turbine. Brake torque must exceed 30,400 lb-ft of wind torque to slow the turbine. A brake torque of 45,000 lb-ft is selected as reasonable because the turbine and transmission must be designed to stop the turbine one time without damage in an engineered stop. To determine stop time at a brake torque of 45,000 lb-ft, the inertial energy must be absorbed at the same time as the wind energy. This can be determined as follows:

$$U_b \text{ brake energy} = \frac{\text{brake torque (lb-ft x avg rpm)}}{5252} \times 550 \frac{\text{ft-lb}}{\text{s}} \times \frac{\text{stopping time}}{\text{s}} \quad \text{(B6)}$$

$$U_w \text{ wind energy} = \frac{\text{wind torque (lb-ft x avg rpm)}}{5252} \times 550 \times t \quad \text{(B7)}$$

or

$$U_b = \frac{45{,}000 \times 31.5}{5252} \times 550 \times t = 148{,}443\ t$$

$$U_w = \frac{30{,}400 \times 31.5}{5252} \times 550 \times t = 100{,}282\ t$$

$$\text{Then } U_b \text{ brake energy} - U_w \text{ wind energy} = \text{inertial energy}, \quad \text{(B8)}$$

or

$$(148{,}443 - 100{,}282)t = 832{,}000$$

where

$t = 17.28$ s

$U_b = 2{,}564{,}410$ ft-lb = 3296 Btu

By using the same 1-in. thick steel disk as that used for the clutch and squeezing the disk with a caliper on both sides, disk temperatures can be determined by the following equation and by Fig. B2.[5]

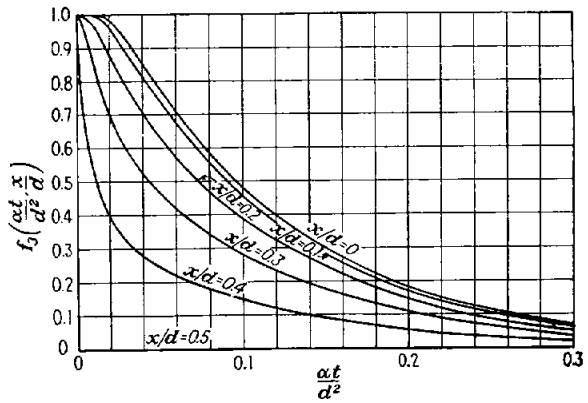

Figure B2. Brake Temperature Function*

$$\theta = \theta_s - (\theta_s - \theta_o)\, f_3\left(\frac{\alpha t}{d^2}, \frac{x}{d}\right)^\circ F \qquad \text{(B9)}$$

where

θ = temperature, at distance x from disk center ($^\circ$F)

θ_s = heated surface temperature ($^\circ$F)

θ_o = starting temperature ($^\circ$F)

x = distance from disk center (ft)

t = time (hr)

α = thermal diffusivity (ft^2/hr)

Since emergency stop time is 17.28 and the brake disk is heated from both sides, the disk achieves a center temperature of 370°F with a surface temperature of 400°F and absorbs 1463 Btu/ft^2. An area of 2.25 ft^2 is necessary to absorb the 3296 Btu required to stop the VAWT.

*Reprinted by permission of McGraw-Hill Book Company from p. 198 of Ref. 5.

Figure B3 shows the maximum diameters of steel disks, diameters that are limited

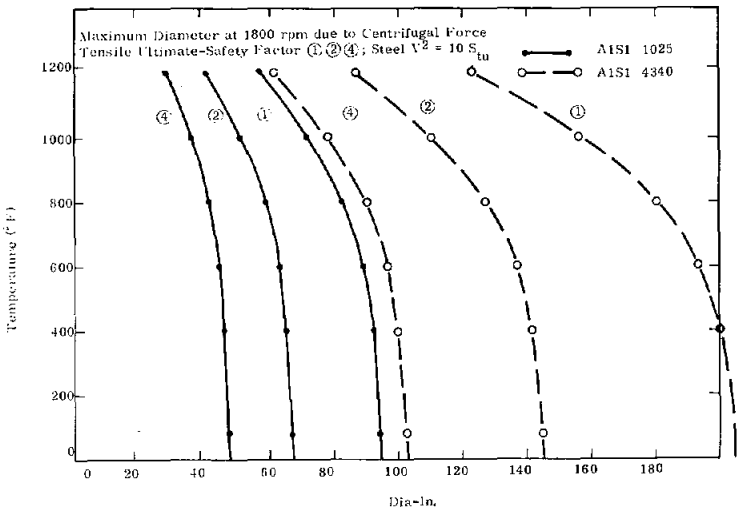

Figure B3. Brake Disk Diameter

because of centrifugal force at 1800 rpm vs temperature. This force, besides limiting the possible disk diameters of brakes and clutches, can require the use of multiple disks for a design, depending upon the design ground rules applied.

Figure B4 shows the differential temperature limit for steel brake disks. The thermal stress created by heating the steel brake disk during start and stop is given by the following equation:

$$S_y = E\gamma\Delta T \tag{B10}$$

where

S_y = yield stress (psi)
E = modulus of elasticity (psi)
γ = coefficient of thermal expansion (in./in.°F)
ΔT = differential temperature (°F)

With the starting temperature of 100°F and a final temperature of 400°F, the clutch calculations show that the hub area will not change temperature during the stopping time. This gives a differential temperature in the brake disk of 300°F.

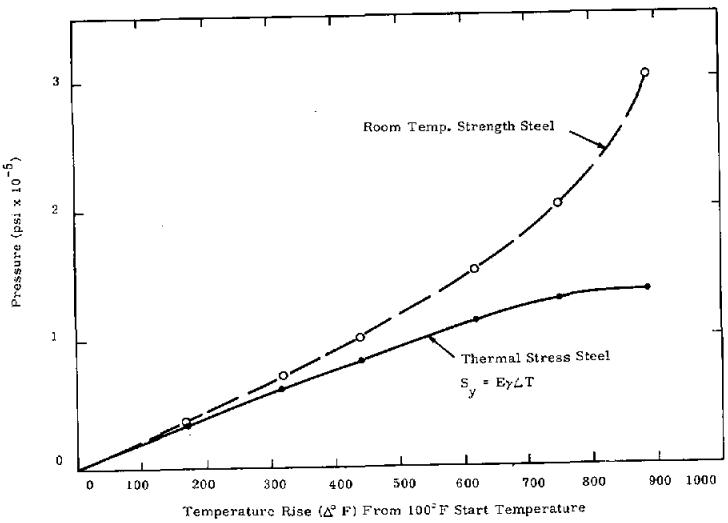

Figure B4. Brake Disk Thermal Stress

Since yield strength decreases faster with increased temperature than does the modulus of elasticity, the modulus of elasticity at the final temperature of 400°F is used. The average coefficient of thermal expansion from 100°F to 400°F is used. This gives the following thermal stress in the brake disk during the stopping operation:

$$S_t = 27.55 \times 10^6 \times 7.1 \times 10^{-6} \times 300 = 58{,}700 \text{ psi} \qquad \text{(B11)}$$

APPENDIX C

Structural Constraints

APPENDIX C
Structural Constraints

The major structural components of the vertical-axis WECS (the blades, tower, and tiedown cables) are constrained dimensionally in the optimization model to ensure compliance with minimum structural performance standards.

Several simplifying assumptions were made in establishing these constraints, as it is not possible to complete a complex structural analysis of each component within the optimization model. Thus, while the constraints do screen out designs that clearly are structurally inadequate, they are not intended to eliminate subsequent detailed structural analyses on each point design.

Structural constraints have a substantial impact on the overall optimization study because the basic dimensions (and hence the costs) of the rotor components are governed by the structural constraints. It is therefore recommended that this area receive attention in future research programs, with attention directed toward the refinement and confirmation of existing calculations.

Blade Structural Constraints

The structural adequacy of a blade is a function of its chord, the mechanical inertias and area of the cross section, the rotor diameter and H/D ratio, and the physical properties (yield strength, elastic modulus, etc) of the blade material. To limit the large number of possible variations among these blade characteristics, this study is restricted to aluminum extrusions of 6063-T5 material. A simplified cross section is used to calculate section properties. This section is simply a NACA 0015 hollow airfoil with uniform wall thickness (Fig. C-1). Of course, extruded blades designed for this application typically have vertical webs to stabilize the forming of curved blade sections, but these vertical webs have only a small influence on cross-section inertias. The advantage to this simple section is that mechanical cross-section properties may be very easily calculated from the blade chord, C, and the wall thickness-to-chord ratio, r = t/C. Table C-I summarizes the simple calculations required to determine all the section properties for the blade.

A set of minimum acceptable performance criteria is required to establish structural adequacy of the blade. The following criteria have been used in the optimization model:

1. Vibratory trailing edge blade stresses because of edgewise blade loading less than the endurance limit at a normal operating condition of 150-fps tipspeed with 60-mph winds.

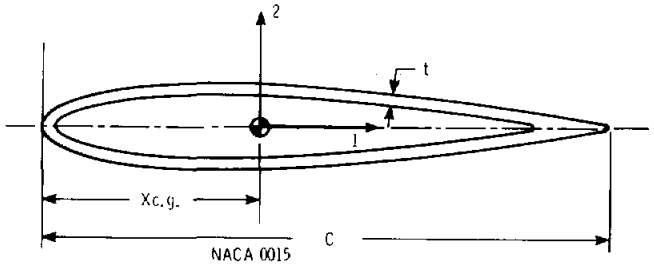

C BLADE CHORD
t BLADE WALL THICKNESS
Xc.g. DISTANCE FROM NOSE TO CENTROID
I_E EDGEWISE SECTION INERTIA = I_{22}
I_F FLATWISE SECTION INERTIA = I_{11}
J TWISTING STIFFNESS FORM FACTOR

Figure C-1. Blade Model for Determining Structural Constraints

TABLE C-I

Property Values for Simplified Blade Section in Fig. C-1

Quantity	Value
Flatwise Inertia I_F	$c^4 r\ 6.2 \times 10^{-3}$
Edgewise Inertia I_E	$c^4 r\ 1.7 \times 10^{-1}$
Twisting Stiffness to Edgewise Stiffness Ratio GJ/EI_E	0.036
Blade Centroid Location X_{cg}	0.49 C
Structural Area A_s	$2.08\ c^2 r$
Enclosed Area	$0.102\ c^2$

Notes: Units of structural quantities are determined by the units of blade chord, C; r is the ratio of wall thickness-to-blade chord.

Property calculations use thin-wall approximations and should not be used for $r > 0.015$.

2. Twisting deformations in the blade because of edgewise loading less than 2 degrees at the normal operating condition.
3. No blade collapse with a parked rotor with 150-mph centerline windspeeds normal to the blade chord.
4. Gravitational stresses less than 40% of yield (assumed to be 30,000 psi) in the parked, wind-off condition.
5. Flatwise stresses because of centrifugal and aerodynamic loads below the endurance limit at the normal operating condition.

The endurance limit for the vibratory blade stresses is taken to be 6000 psi (zero to peak) for the 6063-T5 extrusions. This is a very conservative estimate[6] for a 10^7 cycle lifetime. Considering the infrequent nature of 60-mph winds, and the fact that vibratory stresses decrease to zero as windspeed is reduced,[7] the 10^7 cycle fatigue lifetime corresponds to considerably more actual rotor cycles.

There are, of course, many other structural criteria involved in designing a Darrieus rotor blade, but a blade design that meets these fairly severe criteria will in all likelihood be structurally acceptable. Notable in their absence as structural criteria are blade resonant frequency requirements; this is because the above conditions lead to blades that necessarily are quite stiff in both the flatwise and edgewise directions. This produces relatively high blade resonant frequencies, the order of two to three times the rotational frequency of the rotor. While these frequencies are not high enough to preclude significant aerodynamic excitation of blade resonances, the probability of such excitation is low. Also, the frequency spacing between the lowest blade modes is large enough to avoid any excitations that may occur by making small adjustments to the synchronous rotor rpm.

Given the structural performance requirements on the blade, it remains to estimate stress levels as a function of blade structural properties. This has been done by extending results from finite-element analyses[8] of the 17-m research turbine. Dimensional analysis is used to deduce performance of geometrically similar rotors with different blade properties. An example of this approach is shown in Fig. C-2. Results for the edgewise bending stress* at the blade root are expressed in dimensionless form. The dimensionless stress is

$$\sigma_b/(R^2 V_{max} L/I_e) \quad ,$$

*Edgewise bending stresses are estimated with quasistatic loading; i.e., dynamic effects are neglected. This procedure is justified if blade and system resonant frequencies are well above the aerodynamic excitation frequencies. If this is not the case, the result should be interpreted cautiously.

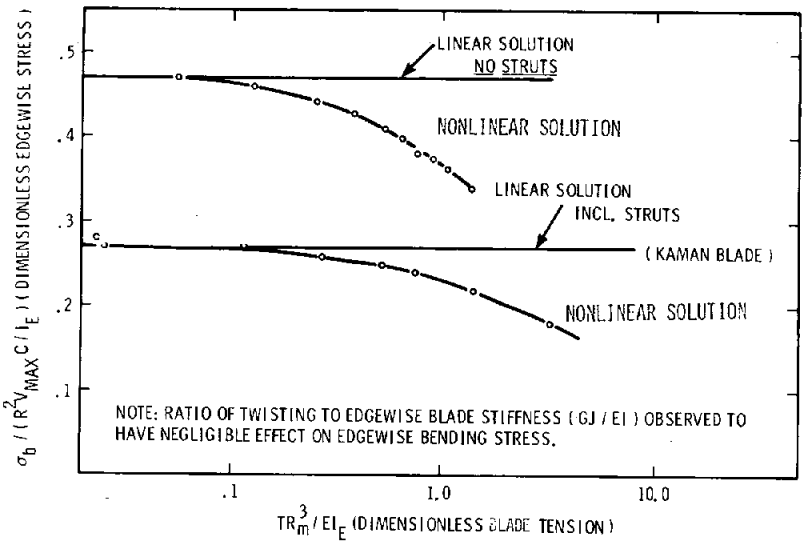

Figure C-2. Edgewise Bending Stress as a Function of Blade Tensile Load, T

where σ_b is the dimensional stress, R is the turbine radius, V_{max} is the edgewise aerodynamic loading per foot of blade at the rotor centerline, L is the distance from the centroid of the blade to the trailing edge, and I_e is the cross-section edgewise moment of inertia. Two cases are shown for rotors with or without 17-m-type support struts. A centrifugal stiffening effect is shown in Fig. C-2. The amount of centrifugal stiffening depends on the rotationally induced blade tension, T, expressed in dimensionless form. The maximum aerodynamic load, V_{max}, is estimated with the single streamtube model.[9,10] The load, V_{max}, and hence the edgewise bending stress, depend on the wind and tipspeed associated with the operating condition and the turbine geometry. For a fixed set of operational conditions, the load, V_{max}, is almost directly proportional to the blade chord, C.

Similar dimensionless curves have been developed for other aspects of structural performance, including parked-blade gust loading, gravitational stresses and deflections, blade twist due to edge loading, and flatwise blade stresses. These curves are used like the edgewise stress curves to estimate performance of many turbine types.

Blade stress levels and deflections become progressively higher for a fixed ratio of blade wall thickness-to-chord length as the chord-to-radius ratio (C/R) is reduced. This is because blade cross-section properties deteriorate rapidly with reduced chord (see Table C-I). Thus, there is some minimum value of C/R at which the structural performance is just adequate. Because of the dependence of the blade section properties

on the blade wall thickness-to-chord ratio, r = t/C, this minimum possible C/R depends on r.

A curve of minimum possible C/R's as a function of r (Fig. C-3) is shown for

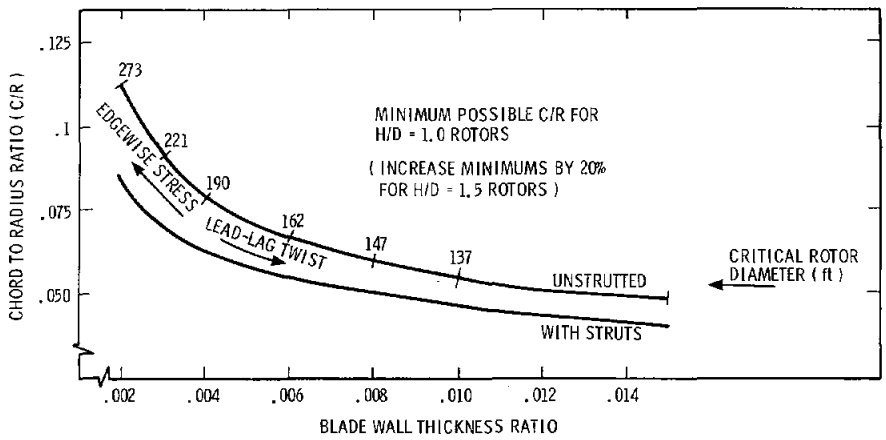

Figure C-3. Chord-to-Rotor Radius Ratio Minimums as a Function of Blade Wall Thickness

rotors with an H/D ratio of 1. The structural criterion that is first violated at the minimum C/R is indicated on the figure. Note that for large wall thickness-to-chord ratios, the blade twist condition is dominant, while thinner walled blades are vulnerable to edgewise stresses. Also indicated on the figure is a critical rotor diameter, the rotor diameter above which gravitational stress condition is violated. The critical diameter may be increased by increasing the blade C/R.

Modifying the definition of minimum acceptable performance will naturally change the minimum possible C/R. Examination of performance criteria indicates that the first four criteria are dominant and or nearly equal importance. Thus, a significant change in minimum possible C/R would require reduction in the performance standards on all of the first four conditions.

Note that the results shown in Fig. C-3 are only valid approximations for the aluminum extruded blade section of Fig. C-1. Using other materials or a different section geometry may change the minimum possible C/R.

Support struts as used on the DOE/Sandia and the Canadian National Research Council (NRC) Magdalen Island turbines tend to decrease the minimum possible C/R because the struts contribute to improved edgewise stiffness, parked buckling resistance, and reduced gravitational stresses. This effect is indicated on Fig. C-3,

based on analyses of the strutted 17-m turbine. The critical diameters for gravitational loads are not shown on this figure because they are generally above 500 ft and out of the range of interest in this study.

For a blade of given chord and wall thickness, rotors with larger H/D ratios are expected to be weaker in all directions because of the increased aspect ratio (blade length-to-chord ratio) of the blades. In analyzing H/D > 1 rotors in the optimization model, the minimum permissible C/R has been increased 20% to account for this effect. This increase is a judgmental estimate that is currently being examined with new finite element models for H/D = 1.5 rotors.

Tower Structural Constraints

The tower is defined as the rotating support structure between the upper tiedown bearing and the base support above the transmission. It is a single tube designed to transmit aerodynamic torque from the blades and axial tiedown reactions into the transmission. Tower construction is assumed to be of mild steel with a cylindrical cross-section and uniform wall thickness.

The following structural criteria, based on the formulas in Table C-II, are used to evaluate towers:

1. General and local buckling loads are at least 10 times greater than tower axial loads.
2. Torsional and bending tower natural frequencies are above 4/rev at a rotor tip speed of 200 fps.
3. Tower axial stresses are below 6,000 psi.

Generally, these conditions are in decreasing order of dominance. The buckling condition safety factors are high to account for eccentricities and local flaws in the structure that inevitably occur in any real design.

The basic structural parameters involved in tubular tower selection are the tower diameter and its wall thickness. Many possible combinations of these parameters can satisfy the structural criteria; however, a unique combination resulted if the requirement of minimum tower volume (weight) was added. Such minimum volume towers are used in the optimization model.

Although the tower dimensions resulting from application of this model do meet structural requirements, they may violate other practical considerations. For example, a tower diameter should not be a substantial fraction of the rotor diameter, or flow blockage may occur. Excessively thin or thick walls may be difficult or impossible to manufacture These special problems require some user care in interpretation of results to avoid conflicts.

TABLE C-II

Formulas Used for Determining Tower Performance

Critical general buckling load, P_{crg}:

$$P_{crg} = \left(\frac{\pi^3 E}{64L^2}\right) D_o^4[1 - (D_i/D_o)^4]$$

Critical local buckling load, P_{crl}:

$$P_{crl} = \left(\frac{\pi E}{4\sqrt{3(1 - \nu^2)}}\right) D_o^2(1 - D_i/D_o)[1 - (D_i/D_o)^2]$$

First tower bending frequency, f_b:

$$f_b = .39\sqrt{E/\rho L^4}\, D_o[1 + (D_i/D_o)^2]^{\frac{1}{2}}$$

First tower torsional frequency, f_t:

$$f_t = (G/\pi L J_b)^{\frac{1}{2}} D_o^2[1 - (D_i/D_o)^4]^{\frac{1}{2}}$$

Static compressive stress, σ_c:

$$\sigma_c = \text{net axial load}/(\pi/4)\, D_o^2[1 - (D_i/D_o)^2]$$

where

D_o = tower OD

D_i = tower ID

L = tower length

E = Young's modulus

G = shear modulus

ν = Poisson's ratio

J_b = polar mass moment of inertia of tower and blades

The mechanics of calculating tower dimensions are automatically carried out in the optimization model. Axial tower load sources accounted for include the tiedown reactions, the axial component of centrifugal blade loads, and the weight of the tiedowns, tower, and blades. The tower length is calculated from the rotor geometry, including any additional ground clearance specified by the user. The formulas in Table C-II are used to calculate critical buckling loads, resonant frequencies, and stresses.

Typical results for minimum volume, structurally adequate tower dimensions are shown in Fig. C-4. It is noteworthy that the tower proportions suggested by this

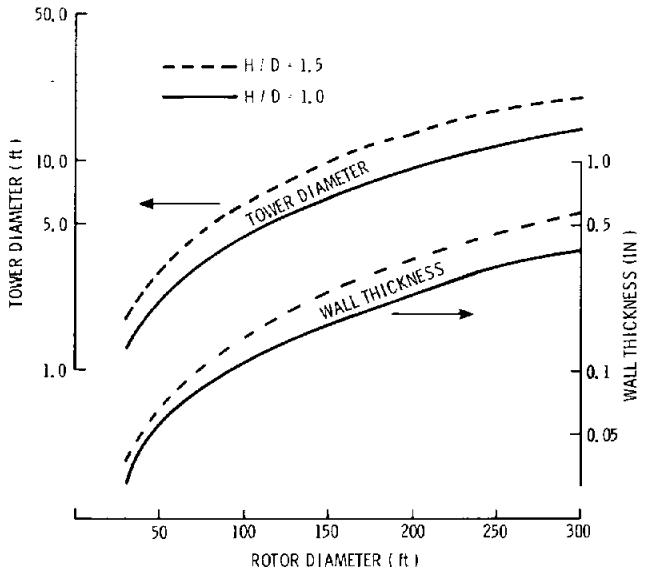

Figure C-4. Dimensions of Minimum Volume Towers Satisfying the Structural Criteria Discussed in the Tower Structural Constraints Section

model have larger diameters and much thinner walls than were used on the Sandia 5-m and 17-m prototypes. These large diameter, thin-walled towers are substantially lighter than the smaller diameter, thick-walled tubes used in the past.

Tiedown Structural Constraints

The cable tiedown system provides a simple, inexpensive way to support the rotor against overturning loads. Two properties of the cable are subject to structural constraints -- the cable diameter and the pretension. The cable diameter has direct impact on cable cost; the pretension influences tower and foundation costs.

The structural constraints imposed in the optimization model are derived from a scaling analysis of the 17-m research turbine cable system.[11,12] A major exception to this rule is the use of three cables in this study rather than the four used on the 17-m system. This change was made to simplify and reduce the amount of material in the tiedown system.

In selection of cable size, the diameter was chosen in the same proportion to cable length as that on the 17-m turbine. This yields a dynamically similar stiffness on top of the tower regardless of absolute rotor size.

Selecting the pretension is more complex. Pretension is required because of cable droop, which occurs in the downwind cable when the tower is loaded by aerodynamic blade forces. This droop drastically reduces the effective stiffness of the downwind cable and increases the possibility of a blade striking a cable. In the optimization model, the pretension is chosen so that the loss of downwind cable stiffness is less than 20% of the full, no-droop stiffness. The loading condition used for this requirement is a "normal" operating case, with the rotor at 150-fps tipspeed in a 60-mph wind. Satisfying this stiffness requirement generally leads to cable droop displacements < 1% of the cable length.

Results for the cable pretension are shown in Fig. C-5 for rotors with H/D's of 1.0 and 1.5. To satisfy the droop requirements, the pretension increases with rotor diameter to approximately the 2-1/3 power. Since cable strength grows with the square of the rotor diameter, there is some limiting size on tiedown systems designed to these pretension conditions. This effect is shown in Fig. C-5 where the cable safety factor, defined as the ratio of cable ultimate strength to maximum working load, steadily decreases with increasing rotor diameter. However, for rotor diameters of < 300 ft, safety factors are still adequate.

Also shown in Fig. C-5 is the first resonant frequency of the cable expressed as a multiple of the rotational frequency of the rotor. This curve is approximate in that the rotor frequency is estimated for normal operating conditions based on a 150-fps tipspeed operating condition.

An actual turbine may differ in rotor speed from this estimate by 20% because of differences in rotor solidity or site wind characteristics. The fundamental excitation frequency into the cables is n per rev, where n is the number of blades. It is evident that H/D = 1.5 rotors with two blades will excite the cables above the first cable frequency. Alternatively, for H/D = 1.0; two-bladed systems provide excitation below the first cable resonance. It is believed, based primarily on experience with the 17-m rotor, that either case can produce acceptable cable performance although some fine tuning of the rotor rpm and/or cable tension may be required.

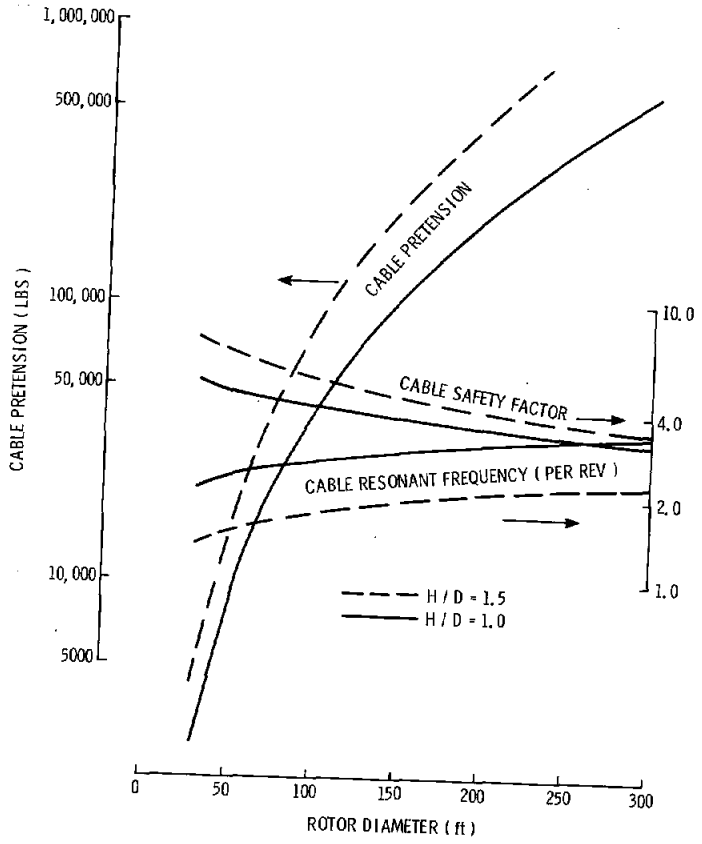

Figure C-5. Cable Pretension, Resonant Frequency, and Safety Factor as a Function of Rotor Diameter

The prescribed cable tensions can have a considerable effect on system costs because of their influence on the tower sizing, rotor bearing requirements, and foundation loads. The pretension rules discussed have been successfully applied to the DOE/Sandia 17-m rotor, but they are believed to be conservative. For example, the Canadian Magdalen Island rotor has roughly half the pretension indicated in Fig. C-5. Future research directed toward establishing less conservative, lower tension design guidelines is advisable.

References

1. G. E. Reis and B. F. Blackwell, Practical Approximations to a Troposkien by Straight-Line and Circular-Arc Segments, SLA74-0100, Sandia Laboratories, Albuquerque, NM, March 1975.

2. B. F. Blackwell and G. E. Reis, Blade Shape for a Troposkien-Type of Vertical Axis Wind Turbine, SLA74-0154, Sandia Laboratories, Albuquerque, NM, April 1974.

3. "Cost Study - Vertical Axis Wind Turbine Power Conversion Systems for Sandia Laboratories," Stearns-Roger Engineering Co., Denver, CO, under Contract No. 05-6105, September 1977.

4. H. E. Auld and P. F. Lodde, A Study of Foundation/Anchor Requirements for Prototype Vertical Axis Wind Turbines, SAND78-7046, Civil Engineering Research Facility of the University of New Mexico, for Sandia Laboratories, Albuquerque, NM, February 1979.

5. A. I. Brown and S. M. Marco, Introduction to Heat Transfer, McGraw-Hill Book Company, New York, 1942.

6. Kaman Aerospace Corporation, private communication.

7. W. N. Sullivan, Preliminary Blade Strain Gage Data on the Sandia 17 Meter Vertical Axis Wind Turbine, SAND77-1176, Sandia Laboratories, Albuquerque, NM, December 1977.

8. L. I. Weingarten and D. W. Lobitz, "Blade Structural Analysis," Vertical Axis Wind Turbine Technology Workshop, SAND76-5586, Sandia Laboratories, Albuquerque, NM, May 17-20, 1976.

9. J. H. Strickland, The Darrieus Turbine: A Performance Prediction Model Using Multiple Streamtubes, SAND75-0431, Sandia Laboratories, Albuquerque, NM, October 1975.

10. W. N. Sullivan, "Structural Loads for the 17-m Darrieus Turbine," Vertical Axis Wind Turbine Technology Workshop, SAND76-5586, Sandia Laboratories, Albuquerque, NM, May 17-20, 1976.

11. R. C. Reuter, Jr., Vertical Axis Wind Turbine Tiedown Design With an Example, SAND77-1919, Sandia Laboratories, Albuquerque, NM, December 1977.

12. R. C. Reuter, Jr., Tiedown Cable Selection and Initial Tensioning for the Sandia 17 Meter Vertical Axis Wind Turbine, SAND76-0616, Sandia Laboratories, Albuquerque, NM, February 1977.

DISTRIBUTION:

TID-4500-R66 UC-60 (283)

Aero Engineering Department (2)
Wichita State University
Wichita, KS 67208
Attn: M. Snyder
W. Wentz

Dr. Daniel K. Ai
Senior Scientific Associate
Alcoa Laboratories
Aluminum Company of America
Alcoa Center, PA 15069

R. E. Akins, Assistant Professor
Department of Engineering Science
and Mechanics
Virginia Polytechnic Institute and
State University
Blacksburg, VA 24060

Mr. Robert B. Allen
General Manager
Dynergy Corporation
P.O. Box 428
1269 Union Avenue
Laconia, NH 03246

American Wind Energy Association
54468 CR31
Bristol, IN 46507

E. E. Anderson
South Dakota School of Mines
and Technology
Department of Mechanical Engineering
Rapid City, SD 57701

Scott Anderson
318 Millis Hall
University of Vermont
Burlington, VT 05405

George W. Barnes
Barnes Engineering Co.
1645 South Claudina Way
Anaheim, CA 92805

F. K. Bechtel
Washington State University
Department of Electrical Engineering
College of Engineering
Pullman, WA 99163

M. E. Beecher
Arizona State University
Solar Energy Collection
University Library
Tempe, AZ 85281

K. Bergey
University of Oklahoma
Aero Engineering Department
Norman, OK 73069

Dr. B. F. Blackwell
Department of Mechanical Engineering
Lousisiana Tech University
Ruston, LA 71270

Steve Blake
Wind Energy Systems
Route 1, Box 93-A
Oskaloosa, KS 66066

Robert Brulle
McDonnell-Douglas
P.O. Box 516
Department 241, Building 32
St. Louis, MO 63166

R. Camerero
Faculty of Applied Science
University of Sherbrooke
Sherbrooke, Quebec
CANADA J1K 2R1

Professor V. A. L. Chasteau
School of Engineering
University of Auckland
Private Bag
Auckland, NEW ZEALAND

Howard T. Clark
McDonnell Aircraft Corporation
P.O. Box 516
Department 337, Building 32
St. Louis, MO 63166

Dr. R. N. Clark
USDA, Agricultural Research Service
Southwest Great Plains Research Center
Bushland, TX 79012

Arthur G. Craig
Alcoa Mill Products
Alcoa Center, PA 15069

Dr. D. E. Cromack
Associate Professor
Mechanical and Aerospace Engineering
Department
University of Massachusetts
Amherst, MA 01003

DOE/ALO (3)
Albuquerque, NM 87185
Attn: D. K. Nowlin
W. P. Grace
D. W. King

DOE Headquarters (20)
Washington, DC 20545
Attn: L. V. Divone, Chief
Wind Systems Branch
G. T. Tennyson, Program Manager
Wind Systems Branch
D. F. Ancona, Program Manager
Wind Systems Branch

C. W. Dodd
School of Engineering
Southern Illinois University
Carbondale, IL 62901

D. P. Dougan
Hamilton Standard
1730 NASA Boulevard
Room 207
Houston, TX 77058

J. B. Dragt
Nederlands Energy Research Foundation (E.C.N.)
Physics Department
Westerduinweg 3 Patten (nh)
THE NETHERLANDS

C. E. Elderkin
Battelle-Pacific Northwest Laboratory
P.O. Box 999
Richland, WA 99352

Frank R. Eldridge, Jr.
The Mitre Corporation
1820 Dolley Madison Blvd.
McLean, VA 22102

Electric Power Research Institute
3412 Hillview Avenue
Palo Alto, CA 94304
Attn: E. Demeo

James D. Fock, Jr.
Department of Aerospace Engineering Sciences
University of Colorado
Boulder, CO 80309

Albert Fritzsche
Dornier System GmbH
Postfach 1360
7990 Friedrichshafen
WEST GERMANY

W. W. Garth, IV
Tyler & Reynolds & Craig
One Boston Place
Boston, MA

E. Gilmore
Amarillo College
Amarillo, TX 79100

Roger T. Griffiths
University College of Swansea
Department of Mechanical Engineering
Singleton Park
Swansea SA2 8PP
UNITED KINGDOM

Professor N. D. Ham
Massachusetts Institute of Technology
77 Massachusetts Avenue
Cambridge, MA 02139

Sam Hansen
DOE/DST
20 Massachusetts Avenue
Washington, DC 20545

W. L. Harris
Aero/Astro Deprtment
Massachusetts Institute of Technology
Cambridge, MA 02139

Terry Healy (2)
Rocky Flats Plant
P.O. Box 464
Golden, CO 80401

Helion
P.O. Box 4301
Sylmar, CA 91342

Don Hinrichsen
Associate Editor
AMBIO
KVA
Fack, S-10405
Stockholm
SWEDEN

J. T. Huang
Alcoa Laboratories
Aluminum Company of America
Alcoa Center, PA 15069

Sven Hugosson
Box 21048
S. 100 31 Stockholm 21
SWEDEN

O. Igra
Department of Mechanical Engineering
Ben-Gurion University of the Negev
Beer-Sheva, ISRAEL

JBF Scientific Corportion
2 Jewel Drive
Wilmington, MA 01887
Attn: E. E. Johanson

Dr. Gary L. Johnson, P.E.
Electrical Engineering Department
Kansas State University
Manhattan, KS 66506

J. P. Johnston
Stanford University
Department of Mechanical Engineering
Stanford, CA 94305

J. R. Jombock
Alcoa Laboratories
Aluminum Company of America
Alcoa Center, PA 15069

Kaman Aerospace Corporation
Old Windsor Road
Bloomfield, CT 06002
Attn: W. Batesol

Robert E. Kelland
The College of Trades and Technology
P.O. Box 1693
Prince Philip Drive
St. John's, NEWFOUNDLAND
A1C 5P7

Larry Kinnett
P.O. Box 6593
Santa Barbara, CA 93111

O. Krauss
Michigan State University
Division of Engineering Research
East Lansing, MI 48824

Lawrence Livermore Laboratory
P.O. Box 808 L-340
Livermore, CA 94550
Attn: D. W. Dorn

M. Lechner
Public Service Company of New Mexico
P.O. Box 2267
Albuquerque, NM 87103

George E. Lennox
Industry Director
Mill Products Division
Reynolds Metals Company
6601 West Broad Street
Richmond, VA 23261

J. Lerner
State Energy Commission
Research and Development Division
1111 Howe Avenue
Sacramento, CA 95825

L. Liljidahl
Building 303
Agriculture Research Center
USDA
Beltsville, MD 20705

P. B. S. Lissaman
Aeroenvironment, Inc.
660 South Arroyo Parkway
Pasadena, CA 91105

Olle Ljungstrom
FFA, The Aeronautical Research Institute
Box 11021
S-16111 Bromma
SWEDEN

Los Alamos Scientific Laboratories
P.O. Box 1663
Los Alamos, NM 87544
Attn: J. D. Balcomb Q-DO-T
Library

Ernel L. Luther
Senior Associate
PRC Energy Analysis Co.
7600 Old Springhouse Rd.
McLean, VA 22101

L. H. J. Maile
48 York Mills Rd.
Willowdale, Ontario
CANADA M2P 1B4

Frank Matanzo
Dardalen Associates
15110 Frederick Road
Woodbine, MD 21797

J. R. McConnell
Tumac Industries, Inc.
650 Ford St.
Colorado Springs, CO 80915

James Meiggs
Kaman Sciences Corporation
P.O. Box 7463
Colorado Springs, CO 80933

R. N. Meroney
Colorado State University
Department of Civil Engineering
Fort Collins, CO 80521

G. N. Monsson
Department of Economic Planning
and Development
Barrett Building
Cheyenne, WY 82002

NASA
Langley Research Center
Hampton, VA 23665
Attn: R. Muraca, MS317

NASA Lewis Research Center (2)
2100 Brookpark Road
Cleveland, OH 44135
Attn: J. Savino, MS 509-201
R. L. Thomas
W. Robbins
K. Kaza, MS 49-6

V. Nelson
West Texas State University
Department of Physics
P.O. Box 248
Canyon, TX 79016

Leander Nichols
Natural Power, Inc.
New Boston, NH 03070

Oklahoma State University (2)
Stillwater, OK 76074
Attn: W. L. Hughes
EE Department
D. K. McLaughlin
ME Department

Oregon State University (2)
Corvallis, OR 97331
Attn: R. Wilson
ME Department
R. W. Thresher
ME Department

H. H. Paalman
Dow Chemical USA
Research Center
2800 Mitchell Drive
Walnut Creek, CA 94598

R. A. Parmelee
Northwestern University
Department of Civil Engineering
Evanston, IL 60201

Art Parthe
Draper Laboratory
555 Technology Square
Mail Station 22
Cambridge, MA 02139

Helge Petersen
Riso National Laboratory
DK-4000 Roskilde
DENMARK

Dr. Barry Rawlings, Chief
Division of Mechanical Engineering
Commonwealth Scientific and Industrial
Research Organization
Graham Road, Highett
Victoria, 3190
AUSTRALIA

Thomas W. Reddoch
Associate Professor
Department of Electrical Engineering
The University of Tennessee
Knoxville, TN 37916

A. Robb
Memorial University of Newfoundland
Faculty of Engineering and Applied Sciences
St. John's Newfoundland
CANADA A1C 5S7

Dr. L. Schienbein
Development Engineer
DAFINDAL Limited
3570 Hawkestone Rd.
Mississauga, Ontario
CANADA L5C 2V8

Arnan Seginer
Professor of Aerodynamics
Technion-Israel Institute of
Technology
Department of Aeronautical
Engineering
Haifa, ISRAEL

Dr. Horst Selzer
Dipl.-Phys.
Wehrtechnik und Energieforschung
ERNO-Raumfahrttechnik GmbH
Hunefeldstr. 1-5
Postfach 10 59 09
2800 Bremen 1
GERMANY

H. Sevier
Rocket and Space Division
Bristol Aerospace Ltd.
P.O. Box 874
Winnipeg, Manitoba
CANADA R3C 2S4

P. N. Shankar
Aerodynamics Division
National Aeronautical Laboratory
Bangalore 560017
INDIA

David Sharpe
Kingston Polytechnic
Canbury Park Road
Kingston, Surrey
UNITED KINGDOM

D. G. Shepherd
Cornell University
Sibley School of Mechanical and
Aerospace Engineering
Ithaca, NY 14853

Dr. Fred Smith
Mechanical Engineering Department Head
Colorado State University
Ft. Collins, CO 80521

Leo H. Soderholm
Iowa State University
Agricultural Engineering, Room 213
Ames, IA 50010

Howard Sonksen
18600 Main St.
Huntington Beach, CA 92648

Southwest Research Institute (2)
P.O. Drawer 28501
San Antonio, TX 78284
Attn: W. L. Donaldson, Senior Vice President
R. K. Swanson

Rick Stevenson
Rt. 10
Box 830
Springfield, MO 65803

Dale T. Stjernholm, P.E.
Mechanical Design Engineer
Morey/Stjernholm and Associates
1050 Magnolia Street
Colorado Springs, CO 80907

R. J. Templin (3)
Low Speed Aerodynamics Section
NRC-National Aeronautical Establishment
Ottawa 7, Ontario
CANADA K1A OR6

Texas Tech University (3)
P.O. Box 4289
Lubbock, TX 79409
Attn: K. C. Mehta, CE Department
J. Strickland, ME Department
J. Lawrence, ME Department

Fred Thompson
Atari, Inc.
155 Moffett Park Drive
Sunnyvale, CA 94086

United Engineers and Constructors, Inc.
Advanced Engineering Department
30 South 17th Street
Philadelphia, PA 19101
Attn: A. J. Karalis

United Nations Environment Program
485 Lexington Avenue
New York, NY 10017
Attn: I. H. Usmani

University of New Mexico (2)
Albuquerque, NM 87106
Attn: K. T. Feldman
Energy Research Center
V. Sloglund
ME Department

Irwin E. Vas
Solar Energy Research Institute
1536 Cole Blvd.
Golden, CO 80401

P. N. Vosburgh, Development Manager
Alcoa Allied Products
Aluminum Company of America
Alcoa Center, PA 15069

Otto de Vries
National Aerospace Laboratory
Anthony Fokkerweg 2
Amsterdam 1017
THE NETHERLANDS

R. Walters
West Virginia University
Department of Aero Engineering
1062 Kountz Avenue
Morgantown, WV 26505

E. J. Warchol
Bonneville Power Administration
P.O. Box 3621
Portland, OR 97225

D. F. Warne, Manager
Energy and Power Systems
ERA Ltd.
Cleeve Rd.
Leatherhead
Surrey KT22 7SA
ENGLAND

R. J. Watson
Watson Bowman Associates, Inc.
1280 Niagara St.
Buffalo, NY 14213

R. G. Watts
Tulane University
Department of Mechanical Engineering
New Orleans, LA 70018

Pat Weis
Solar Energy Research Institute
1536 Cole Blvd.
Golden, CO 80401

W. G. Wells, P.E.
Associate Professor
Mechanical Engineering Department
Mississippi State University
Mississippi State, MS 39762

T. Wentink, Jr.
University of Alaska
Geophysical Institute
Fairbanks, AK 99701

West Texas State University
Government Depository Library
Number 613
Canyon, TX 79015

Wind Energy Report
Box 14
104 S. Village Ave.
Rockville Centre, NY 11571
Attn: Farrell Smith Seiler

C. Wood
Dominion Aluminum Fabricating Ltd.
3570 Hawkestone Road
Mississauga, Ontario
CANADA L5C 2V8

1000 G. A. Fowler
1200 L. D. Smith
3141 T. L. Werner (5)
3151 W. L. Garner (3)
For DOE/TIC (Unlimited Release)
3161 J. E. Mitchell (15)
3161 P. S. Wilson
4533 J. W. Reed
4700 J. H. Scott
4710 G. E. Brandvold
4715 R. H. Braasch (100)
4715 R. D. Grover
4715 E. G. Kadlec
4715 R. O. Nellums
4715 W. N. Sullivan
4715 M. H. Worstell
5520 T. B. Lane
5521 D. W. Lobitz
5523 R. C. Reuter, Jr.
5523 T. G. Carne
5523 P. J. Sutherland
5600 D. B. Schuster
5620 M. M. Newsom
5630 R. C. Maydew
5632 C. W. Peterson
5632 P. C. Klimas
5633 S. McAlees, Jr.
5633 R. E. Sheldahl
8266 E. A. Aas
DOE/TIC (25)
(R. P. Campbell, 3172-3)